



**HAL**  
open science

## Interconnection salt diapir-allochthonous salt sheet in northern Tunisia: The Lansarine-Baoula case study

Zayneb Amri, Chahreddine Naji, Amara Masrouhi, Olivier Bellier

### ► To cite this version:

Zayneb Amri, Chahreddine Naji, Amara Masrouhi, Olivier Bellier. Interconnection salt diapir-allochthonous salt sheet in northern Tunisia: The Lansarine-Baoula case study. *Journal of African Earth Sciences*, 2020, 170, pp.103876. 10.1016/j.jafrearsci.2020.103876 . hal-02979179

**HAL Id: hal-02979179**

**<https://hal.science/hal-02979179v1>**

Submitted on 31 Aug 2021

**HAL** is a multi-disciplinary open access archive for the deposit and dissemination of scientific research documents, whether they are published or not. The documents may come from teaching and research institutions in France or abroad, or from public or private research centers.

L'archive ouverte pluridisciplinaire **HAL**, est destinée au dépôt et à la diffusion de documents scientifiques de niveau recherche, publiés ou non, émanant des établissements d'enseignement et de recherche français ou étrangers, des laboratoires publics ou privés.

# Journal Pre-proof

Interconnection salt diapir–allochthonous salt sheet in northern Tunisia: The Lansarine–Baoula case study

Zayneb Amri, Chahreddine Naji, Amara Masrouhi, Olivier Bellier



PII: S1464-343X(20)30127-8

DOI: <https://doi.org/10.1016/j.jafrearsci.2020.103876>

Reference: AES 103876

To appear in: *Journal of African Earth Sciences*

Received Date: 13 December 2019

Revised Date: 7 May 2020

Accepted Date: 7 May 2020

Please cite this article as: Amri, Z., Naji, C., Masrouhi, A., Bellier, O., Interconnection salt diapir–allochthonous salt sheet in northern Tunisia: The Lansarine–Baoula case study, *Journal of African Earth Sciences* (2020), doi: <https://doi.org/10.1016/j.jafrearsci.2020.103876>.

This is a PDF file of an article that has undergone enhancements after acceptance, such as the addition of a cover page and metadata, and formatting for readability, but it is not yet the definitive version of record. This version will undergo additional copyediting, typesetting and review before it is published in its final form, but we are providing this version to give early visibility of the article. Please note that, during the production process, errors may be discovered which could affect the content, and all legal disclaimers that apply to the journal pertain.

© 2020 Published by Elsevier Ltd.

1 **Interconnection salt diapir–allochthonous salt sheet in Northern Tunisia: the Lansarine–**  
2 **Baoula case study**

3

4 Zayneb AMRI<sup>a,\*</sup>, Chahreddine NAJI<sup>a</sup>, Amara MASROUHI<sup>b</sup>, Olivier BELLIER<sup>c</sup>

5 <sup>a</sup> *Geo-Resources Laboratory, Water Researches and Technologies Center Borj-Cedria, Carthage University, Faculty*  
6 *of Sciences of Bizerte, Tunisia.*

7 <sup>b</sup> *King Abdulaziz University, Faculty of Earth Sciences, Geo-exploration Techniques Department, Jeddah, Saudi*  
8 *Arabia.*

9 <sup>c</sup> *Aix Marseille Univ, CNRS, IRD, INRAE, Coll France, CEREGE, Aix-en-Provence, France.*

10 \* *Corresponding author: [zayneb.amri.fsb@gmail.com](mailto:zayneb.amri.fsb@gmail.com)*

11

12 **Abstract**

13 Surface and subsurface data are used to illustrate the halokinetic style, structural evolution and  
14 kinematics of the Lansarine–Baouala salt structure in the Alpine domain of Tunisia. It corresponds to a  
15 salt structure showing a large salt canopy overhanging buried diapir. The salt structure is located along  
16 the main fault systems, inherited from the southern Tethyan passive margin periods. The Northern  
17 domain of Tunisia is undergoing diapirism, which has been recognized as active during the Upper Aptian  
18 and Lower Albian periods. Above the diapir apex, salt flows outward and spreads by gravity downslope.  
19 A minibasin has formed during this period of salt outward evacuation. The minibasin has a thickness  
20 practically correlated to the budget of salt evacuation toward the diapiric structure. During Cenozoic  
21 times, compressional deformation stages do not reflect active diapirism. The Lansarine–Baouala salt  
22 structure, consisting of connected salt sheets, was passively transported on the Southeast-verging major  
23 thrusts that are deeply rooted in the salt beneath the Mateur basin. The Northern Atlas of Tunisia  
24 reveals, as many others salt provinces, an interconnection of salt diapirs and significant laterally  
25 spreading allochthonous salt sheets (canopies?). In this domain, the inherited allochthonous Triassic salt  
26 sheets interlayered within recent series and connected to buried diapir have a significant role in the  
27 shallow structural complexity observed in the sedimentary cover during the subsequent contractional  
28 events.

29 **Keys-words:** North Tunisian Atlas; diapir; allochthonous salt sheets; mini-basin; thrust

## 30        **1. Introduction**

31        Rifts and continental margins are usually characterized by salt deposition followed by salt tectonics,  
32        which strongly influence their structural styles (e.g. Talbot et al., 1991; Weijermars et al., 1993; Jackson  
33        and Vendeville, 1994; Hudec and Jackson, 2007; Callot et al., 2012). Salt tectonics is currently recognized  
34        to have a crucial role in the deformation of several geologic systems around the world in both active and  
35        passive margins (e.g. Rowan et al., 2003; Hudec and Jackson, 2007; Alsop et al., 2015; Moragas et al.,  
36        2017). Rift and passive continental margins tectonic style and/or evolution were the subject of new  
37        tectonic concepts developed during the last 40 years (e.g. Bally, 1983; Allen and Allen, 1990; Brune et  
38        al., 2014). These geologic systems are commonly described as dominated by intra-basin growth listric  
39        normal faults in control of an asymmetrical seafloor that is characterized by repetitive depocenters. The  
40        intra-basin faults system is responsible for the basin's geometry that is characterized by hanging-wall  
41        rollovers, rafts, salt-related features and important thickness and facies variations of sedimentary  
42        sequences. These systems are frequently inverted and deformed by subsequent compressions hence  
43        the area is subject to tectonic inversion. The presence of salt is usually involved in the deformation of  
44        several inverted systems such as the Alpine orogens of Europe, the Betics, the Pyrenees, the North  
45        African alpine belts, Zagros (e.g. Canerot et al., 2005; Masrouhi and Koyi., 2012; Callot et al., 2014; Saura  
46        et al., 2015). The early interpretations of salt tectonics that predominated during the first half of the  
47        20th century were also updated by the upsurge of the thrust tectonics models. This evolutionary trend  
48        has modernized salt tectonic concepts. Recent improvement in drilling and seismic technologies led to a  
49        surge of large allochthonous salt on deep water passive margin. Although salt structures are being  
50        recognized as having large overhangs (e.g. Jackson and Talbot, 1989; Talbot et al., 1991; Talbot, 1993),  
51        several hundreds of salt overhangs are known to exist now (e.g. Wu et al., 1990; Talbot, 1993; Fort and  
52        Brun, 2004; Hudec and Jackson, 2004, 2006, 2009) and are confined to only a few of the many  
53        sedimentary basins containing salt (Gulf Coast, Campos basin, Angola margin, Red Sea). Past salt  
54        overhangs are neglected in literature because they are usually comprised within orogens.

55        After a while, the interaction between salt diapir and salt sheets has been studied by several works in a  
56        large proportion of salt provinces: Australia (e.g. Hearon et al., 2015; Rowan et al., 2019), Iran (e.g.  
57        Heydarzadeh et al., 2020), Turkey (e.g. Kergaravat et al., 2016), Central Europe (e.g. Warsitzka et al.,  
58        2019), the Algarve Portuguese basin (e.g. Ramos et al., 2017), Mexico (e.g. Giles and Rowan, 2012), USA  
59        (e.g. Gradmann and Beaumont, 2017) and among others. Processes of mobilization of salt usually assists  
60        gravitationally driven deformation of rock mass associated with this growth. In passive margin setting,

61 during sedimentation a wide range of gravity driven structures in successive depositional events are  
62 generated along the slope. Salt is itself associated to this evolution in which the overburden moves with  
63 gravity spreading driven by the differential load of tectonic blocks (Alsop and Marco, 2014). The half-  
64 graben, which usually characterizes this growth, develops salt diapir in case of sufficient buried  
65 underlying salt budget. When the salt reaches the sea floor, the interaction of several parameters  
66 guides the evolution of the structure such as the rate of salt evacuation versus the sedimentation rate  
67 (Fernandez et al., 2020), the impact of base-salt relief on salt flow (Dooly et al., 2018), Extension versus  
68 sedimentation rate (Allen et al., 2020)...

69 The Maghreb exposes numerous salt structures and is described as one of the largest worldwide salt  
70 provinces. Salt structures are more abundant in the eastern part of this province which corresponds to  
71 the Northern Tunisian Atlas. This 10000 km<sup>2</sup> area exposes more than 40 structures, most of them are  
72 hundred square kilometers structures (Fig. 1). Salt structures in this region have been the subject of  
73 controversial geologic interpretations (e.g. Perthuisot et al., 1988; Vila et al., 1994; Masrouhi et al.,  
74 2014a). In this province, two different types have been proposed to explain the salt growth and  
75 configuration: (1) the salt pierces the overburden and the sequences' thickness is reduced in the limbs  
76 of the structure which define the diapir or dome model (Bolze 1950; Perthuisot 1978; Perthuisot et al.  
77 1998; Jallouli et al. 2005; Benassi et al. 2006). This model corresponds to the means of 1970s ideas  
78 based on buoyancy -driven convection. Halokinetic movement was attributed to autonomous, isotactic  
79 rise of salt and vertical salt movement versus its overburden due to Rayleigh-Taylor instabilities. (2)  
80 Allochthonous salt interpretation (Ghanmi et al. 2001; Vila et al., 2002; Slama et al., 2009; Masrouhi and  
81 Koyi, 2012; Zouaghi et al., 2013) which suggests a setting with salt flowing at the sediment–water  
82 interface through a feeder frequently acknowledged as the normal faulting affecting the sedimentary  
83 cover over the Triassic salt. The normal synsedimentary faults, formed during the thin-skinned  
84 Cretaceous extension of the southern Tethyan passive margin, create a space for salt to reach the  
85 surface during their motion and then flows on the surface, thus defining a salt glacier structures.  
86 Although the interconnection between salt domes–salt glaciers is well documented in many passive  
87 margins, the interconnection between those two types of structures has never been identified in the  
88 Northeastern Maghreb salt province.

89 This study presents such an interconnection for the first time in this province and demonstrates a  
90 reappraisal of the structure and the diapirism growth style with significant allochthonous salt sheet  
91 (canopy?) spreading laterally from the diapir stem during the lower Cretaceous period. We present new

92 surface and subsurface data for both diapir growth and the salt sheet-related structures, which are now  
93 partially obliterated by subsequent Tertiary compressions that need to be considered in the study of salt  
94 tectonics in the Northern African area.

## 95 **2. Geological setting**

### 96 **2.1. Structural framework**

97 The Northern Tunisia Atlas is the eastern segment of the Maghreb folds-thrust belt known as the  
98 Maghrebides chain (Fig. 1). The Maghrebides is an Alpine belt; occupying the Northwestern African  
99 plate, which is related to the Africa–Eurasia convergence during Tertiary–present-day period. After a  
100 long Mesozoic extensional Tethyan period, the positive inversion of the basins in Tunisia is recognized to  
101 operate during Late Cretaceous (Guiraud and Bosworth, 1997; Masrouhi et al., 2008). During the  
102 Cenozoic compressional history, the first significant contractional event is dated as Middle-Late Eocene  
103 and accepted as the Atlassic compression (e.g. Vila et al., 1975; Frizon de Lamotte et al., 2000). The  
104 Atlassic event is well traced by regional unconformity on the entire Tunisian Atlas (Masrouhi et al., 2007;  
105 Gharbi et al., 2015). During the Oligocene–Lower Miocene period, the Atlas domain shows a post  
106 compressional tectonic quiescence stage. The Oligocene–Miocene sequences are deposited in  
107 distinguished sub-basins such as the Numidian Basin and the Medjedra basin. The tectonic setting seems  
108 to be well correlated to the West-Mediterranean geodynamic setting (Corsica–Sardinia and the  
109 Algerian–Provencal Miocene back-arc basin opening (e.g. Vergés and Sàbat, 1999; Frizon de Lamotte et  
110 al., 2009; Roure et al., 2012; Van Hinsbergen et al., 2014). The Oligocene–lower Miocene extension is  
111 caused at the scale of the margin by the retreat of the slab (e.g. Jolivet and Faccenna, 2000; Deverchere  
112 et al., 2005). In the Tunisian Northern Atlas, the paroxysmal compressional event is considered to have  
113 occurred during Middle Miocene to present-day times by several authors (e.g. Dlala, 1992; Chihi, 1992;  
114 El Ghali et al., 2003; Gharbi et al., 2014). All authors who worked in this region agree that this event is  
115 the major compressional tectonic event deforming the Atlassic domain of Tunisia (e.g. Gharbi et al.,  
116 2014; Bahrouni et al., 2014; Soumaya et al., 2015; Masrouhi et al., 2019). The main regional  
117 compression direction was identified by several studies as NW-trending during Miocene-Pliocene and N-  
118 Trending during the Late Pliocene-Quaternary (e.g. Dlala and Hfaiedh, 1993; Billi et al., 2011; Gharbi et  
119 al., 2014; Soumaya et al., 2015). The northern Atlas of Tunisia shows major NE-trending thrust systems,  
120 with three most important traced fronts from North to South being (Fig. 1): the tell thrust range front,  
121 the Teboursouk Thrust Unit Front (TTUF) and the Zoughan-Ressas Thrust Unit Front (ZRTUF). The  
122 structural style of this belt has recently been identified as the result of the inversion of Mesozoic

123 inherited structures of the earlier passive margin basins and/or sub-basins along the south Tethyan  
124 margin (e.g. Jaillard et al., 2017; Naji et al., 2018a; Masrouhi et al., 2019).

125 The inherited system is well linked to the Jurassic and Cretaceous periods with the southern margin of  
126 the Tethys (Boughdiri et al., 2007; Frizon de Lamotte et al., 2013). The long Tethyan evolution generated  
127 major basins from Morocco to Tunisia during the Late Permian–Late Cretaceous (Roure et al., 2012;  
128 Moragas et al., 2016, 2017; Naji et al., 2018a). The long Mesozoic evolution began with Triassic basins  
129 from an epicontinental environment and characterized by evaporitic facies covering the entire Maghreb  
130 sub-basins (e.g. Soto et al., 2017). The Triassic sub-basins frequently display subordinate basalts  
131 preserved in several localities in Tunisia (Laaridhi-Ouazâa, 1994) that are interpreted as the result of rift-  
132 related magmatism (e.g. Mattoussi Kort et al., 2009). During the Jurassic period, a well-documented  
133 main N-trending regional extension was associated to the development of main basins (e.g. Boughdiri et  
134 al., 2007; Saura et al., 2014; Martin-Martin, 2017; Soussi et al., 2017; Moragas et al., 2018). These basins  
135 are subject to significant thickness and facies variations (Peybernes et al., 1994; Boughdiri et al., 2007).  
136 During Early Cretaceous a NE-SW regional tectonic extensional setting became dominant (e.g. Jaillard et  
137 al., 2017; Naji et al., 2018b). This evolution from E-W (present-coordinates) to NW-SE shape is well-  
138 matched to E-W transform faults of the Atlantic that change to NW-SE in the Alpine Tethys (e.g.  
139 Rosenbaum et al., 2002; Masrouhi et al., 2019). During the lower Cretaceous, a paleogeographic  
140 differentiation was established with a continental platform in the south and center and a deep domain  
141 in the north. This differentiation is associated with volcanic and salt structures, all of them characterized  
142 by a passive margin context (e.g. Mattoussi Kort et al., 2009; Masrouhi et al., 2013; Jaillard et al., 2017;  
143 Dhahri and Boukadi, 2017).

144 Halokinetic signature in the Maghreb domain has long been recognized and mostly interpreted as  
145 Cretaceous–related structures (Bolze, 1954; Perthuisot, 1988; Vila et al., 1994; Masrouhi et al., 2014b).  
146 This belt corresponds to one of the largest worldwide salt provinces in which a debate has been active  
147 for decades between two main interpretations i.e. “vertical” diapir structures [autochthonous  
148 emplacement] and salt sheets [allochthonous mobile evaporites emplaced at younger stratigraphic  
149 levels]. This paper presents new data of the LBSS to highlight a new model of relationship between the  
150 allochthonous salt canopy and the autochthonous diapir feeder, in which the relationship is partially  
151 obliterated by Tertiary compressions.

## 152 **2.2. Lithostratigraphic successions**

153 Mesozoic and Cenozoic series outcrop along the LBSS region and comprise sequences from Triassic to  
154 quaternary deposits.

155 The mainly evaporitic Triassic series shows a thickness that varies from 150 to 1000 m. The Jurassic  
156 series consist of classic limestones Oust, Zaghouan, Staa, Zaress and Beni klab Formations (Peybernes et  
157 al., 1996; Boughdiri et al., 2007). These series are reduced in the southern part of the LBSS compared to  
158 their southern equivalent outcropping in the Tunisian Dorsale (Soussi et al., 1999). They vary from 40 to  
159 450 m in outcropping series near the LBSS and include stratigraphic gaps linked to the tilted block  
160 geometry characterizing this margin during Mesozoic times (Naji et al., 2018b). In the northern domain,  
161 the Jurassic reach a 1000m thickness in the Mateur – Ichkeul area (Alouani et al., 2006). In this area, the  
162 Jurassic sequences usually indicate the presence of siliceous radiolarites revealing an important oceanic  
163 depth (Cordey et al, 2005).

164 The Tithonian-Berriasian displays a facies made of debris-flow and mud-flow sandstones and siltstones  
165 sequences. The Valanginian–Hauterivian is made of siliciclastic carbonate usually covered by mixed shelf  
166 deposits that are dated as Hauterivian and defined as Seroula Formation (Peybernes et al., 1996). The  
167 Barremian sequences are described in this region to contain a lower tempestites unit followed by a thick  
168 carbonate unit and topped by storm deposits and black-shales parasequences (Khessibi, 1967, Souquet  
169 et al., 1997). In northern Tunisia, the Valanginian–Aptian series are defined as M'Cherga Formation  
170 (Buroillet, 1956; Ben Ferjani et al., 1990). The Aptian–Early Albian sequences are typically of deep-water  
171 environment made of gray to black marls. They also habitually contain abundant slumps and nodules  
172 features usually interpreted as related deep and irregular sea floor. This period (Aptian–Albian are the  
173 two longest epochs of the lower Cretaceous) is interpreted as displaying the maximum extensional rate  
174 of the Tethyan basin in northern Tunisia (Masrouhi et al., 2014b, Jaillard et al., 2017; Naji et al., 2018a).  
175 Moreover, more than 80% of the salt structures appeared to be active during Aptian–Albian (e.g.  
176 Perthuisot, 1988; Vila et al., 1994; Ghanmi et al., 2001; Masrouhi et al., 2014a).

177 After the lower Cretaceous deposition variation, the northern Tunisian domain shows a late Cretaceous  
178 homogenous facies cover the entire basin with no significant facies variation. The late Cretaceous basin  
179 is mainly consisting of pelagic to hemipelagic facies. The basin reflects a transgression that invaded and  
180 sealed the aforementioned lower Cretaceous configuration. This deposition of the top of former  
181 dislocation is attested by significant thickness variation along the entire basin. The thicknesses vary  
182 considerably from some meters to hundreds of meters for the same interval from an area to another.



183 This period is characterized by homogenous facies with shales, marls and limestones characteristic of  
184 post rift sedimentation (Fig. 2). The post rift sedimentation started in late Cretaceous times and  
185 smoothly sealed tilted blocks geometries, shaped and accentuated during Early Cretaceous by major  
186 synsedimentary normal fault systems. This second cycle shows limestone and marl alternations at the  
187 base dated as Albian–Cenomanian and defined as Fahdene Formation. These sequences are topped by  
188 organic-rich limestones thinly laminated defined as Bahloul member. On the Fahdene Formation, the  
189 Turonian–Early Campanian Aleg Formation is formed by marl and shale with fine-grained limestones  
190 (Burolet, 1956). Upper Cretaceous sequences, defined as Abiod Formation, display Campanian–  
191 Maastrichtian chalky limestones deposits covering the entire basin of Tunisia (Burolet, 1956).

192 The Tertiary consists of the following sequences: marine black shale series dated as Paleocene and  
193 defined as the El Haria Formation. El Haria Formation is frequently overlain by the lower Eocene  
194 Formation made of limestones. Then, middle to upper Eocene thick series of marls and shales  
195 corresponding to the Souar Formation. Due to the tectonic history (large thrust systems), the upper  
196 Eocene does not outcrop in the Lansarine region. Oligocene sequences involve deltaic siliceous  
197 sandstones. The Neogene sediments are made of thick marine Aquitanian–Burdigalian formations. The  
198 upper Miocene–Pliocene sequences are continental strata recognized as the result of the large erosion  
199 during Cenozoic uplifting and cover unconformably the Neogene and Cretaceous Formations.

### 200 **3. Field data and results**

201 The structural analysis based on a study of detailed geologic maps, controlled by field cross-sections.  
202 Interpretations are based on the detailed geological map (1:25 000 scale) from existing data and data  
203 prepared for this study. Work consists also of the use of the existing detailed micropalaeontological data  
204 from the formations, in order to date the lithologies and illustrate the position of the Triassic salt  
205 relative to the surrounding Mesozoic and Cenozoic sequences. the characteristics and behavior of the  
206 contact between salt and other strata is detailed to draw back the nature of salt (vertical diapir and/or  
207 horizontal salt sheet). Fault kinematics analysis is conducted in some areas, to quantify the brittle  
208 deformation and the tectonic regime contemporaneous to the salt body evolution.

209 The ~ 360 km<sup>2</sup> LBSS corresponds to the second largest salt body in the north Tunisian salt province. In  
210 order to highlight the significant variations of the salt geometry in different areas, we will first discuss  
211 the salt contacts in key-zones and then present the structural style by segment.

212 In the northern part of the LBSS, all the southeast part of the Triassic salt body is in contact with  
213 Cretaceous strata. The Triassic salt overlies Albian sequences in the south (Wadi Maiou). In this region,  
214 lower Albian dips  $45^\circ$  to the NW under the Triassic units that are parallel to the Cretaceous layers and do  
215 not show an extrusive character (Fig. 4). The parallelism between salt contact and Albian layers was the  
216 subject of the most curious interpretations by former study of Bolze (1954) which attribute an Albian  
217 age to the Triassic salt. This parallel contact can be mapped along more than 2 km from Wadi Maiou to  
218 Wadi Tell and, regarding the ravinant character, was interpreted as a “conformable contact” between  
219 Triassic salt and Albian Sequences due to an extrusive flow of salt (Masrouhi et al., 2013). This  
220 terminology was used to qualify the bottom or the top contact of the salt sheet that flowed over the sea  
221 water-sediment interface or was covered by later deposition. This contact is genetically different from a  
222 sharp vertical diapiric contact. In the northwestern part, salt is joined in an anticline structure without  
223 the classical complication of salt (Fig. 4). The Jebel Bou Djebbah anticline structure shows once more a  
224 salt with conformable contact and a cretaceous series that plunges under the Triassic sequences.  
225 Northward, in the Wadi El Ahmer locality, an Aptian sequence crops out in the main salt structure. This  
226 outcropping Cretaceous series was initially described and dated by Masrouhi et al. (2013) as an upper  
227 Aptian sequence. For the first time in this region, a work highlighted a fold structure in which Triassic  
228 salt is incorporated in recent series. The Wadi El Ahmer locality shows a NNE-trending anticline structure  
229 including upper Aptian Triassic salt cover sequences (for dating see Masrouhi et al., 2013) without the  
230 typical salt folding. In the middle part of the large salt outcrop, an Aptian sequence was also identified as  
231 the bedrock of the Triassic evaporites (Fig. 4). This anticline shows a “conformable” Triassic contact  
232 (ravinant, glauconitic and reworked Triassic insoluble elements) at a dipping angle of  $30^\circ$  subparallel to  
233 the above Aptian sequences. Far northwest, the Lella Selilia offers an outcrop of salt sheet with a salt  
234 contact subparallel to its cover that is constituted by a normal stratigraphic succession from upper  
235 Aptian to Campanian sequences. In the northeastern part (the Sebaa Regoud) a “lower conformable  
236 contact” (with respect to the salt position) crops out in this entire region.

237 The central part of this structure shows the main salt body of Lansarine in contact with two cretaceous  
238 outcrops i.e. the Ain El Karma Locality and the Jebel Djedaria (Fig. 5): At Ain el Karma, the Triassic salt  
239 covers dark greenish clays with many nodules associated with slumps (a) themselves covering  
240 limestones (b). For 2 km from the south to the north, the base of the Triassic salt is in contact only on  
241 the term (a). This series has long been regarded as overturned middle Albian series by all authors  
242 (Jauzein, 1962; Zargouni, 1975; Perthuisot, 1978). Masrouhi et al. (2013) presents a detailed

243 micropaleontological association in which a distinction has been established with lower Albian in the  
244 base and middle Albian in the upper part, confirming a normal stratigraphic succession. The Jebel  
245 Djedaria shows the only southern outcrop of Cretaceous sequences under the tertiary complex  
246 configuration of the Jebel Lansarine. This locality offers an outcrop showing a reduced Cretaceous  
247 sequence (compared to their equivalents in northern Tunisia) covering Triassic salt. This section is  
248 formed by Upper Albian to Santonian sequences with normal lithostratigraphic polarity. Thickness and  
249 contact nature (glauconitic, transgressive and phosphatic) testify to a transgressive Cretaceous  
250 sequence on an existing submarine salt sheet that was extruded on a water–sediments interface. The  
251 interbedded position confirms a rapid salt spreading (1 to 2 Ma). Moreover, the Lansarine central part  
252 shows a 500m thick Triassic salt sequence in the East (Ain Karma) and 150 m thick sequences in the  
253 Jebel Kef Debba (Fig. 5), possibly indicating a northwestward thinning of salt and thus a possible  
254 northwestward spreading.

255 The LBSS corresponds to the second largest Triassic salt body in contact with only a few Mesozoic  
256 outcrops, making the interpretation of this structure difficult. The geologic maps and field data (Figs. 3-  
257 6) display evidences that the LBSS is a curved deformed zone bounded mainly by NE- to E-trending faults  
258 systems. Its northern side is affected by the 8-km long N40°E-trending Baouala fault. In the main salt  
259 body this fault is well identified by microfolding along the fault trace. Along the southeastern side of the  
260 Jebel Malouia this fault is confirmed as the main thrust in this region, delimiting a hanging-wall with  
261 Triassic salt and a footwall formed by Campanian to Miocene sequences. The offset is estimated to be  
262 between 1 and 2 km, regarding the salt position versus the Cretaceous sequences and Miocene  
263 sequences. This thrust bounds two varied domains in relation to the salt position: to the northwest the  
264 Triassic salt overlies upper Aptian (described afore in Wadi el Marir, Wadi Ahmer, Jebel Bou Djebbah  
265 and Sebbaa Regoud) and to the southwest salt overlies Albian sequences (Wadi Maiou). The folding  
266 curves and the related structures attest a post Miocene shortening. Three fault sites in this region were  
267 analyzed and display a major NW-SE Miocene to quaternary compression state. Using the fault diagram  
268 (Fig. 4), the first site (sf\_1) indicates a compressional tectonic regime locally characterized by N337°-  
269 trending maximum stress axis ( $\sigma_1$ ). The second site (sf\_2) measured in the Campanian limestone  
270 forming the footwall of the Baouala thrust indicates a similar compressional tectonic regime locally  
271 characterized by N145°-trending maximum stress axis ( $\sigma_1$ ). The third site (sf\_3) measured in the  
272 Miocene limestones also indicates a compressional tectonic regime locally characterized by N343°-  
273 trending maximum stress axis ( $\sigma_1$ ). These three sites are compatible with the majority of the tectonic  
274 studies in northern Tunisia illustrating a NW-trending Miocene to present day main compression (e.g.

275 Melki et al, 2011; Soumaya et al., 2015; Booth-Rea et al., 2018). The fault kinematics analysis is  
276 compatible with field data illustrating a southeast verging of the Baouala thrust.

277 The Lansarine region of northern Tunisia shows a plateau with horizontal Eocene sequences resting on a  
278 well-outcropping marine Miocene series on its southern side and overlapping a detritic series of the  
279 Fortuna formation commonly attributed to the Oligocene (Fig. 6). The Fig.6 shows the configuration and  
280 reproduces the geological history of this region. The Oligocene–lower Miocene sequences cover a  
281 Cretaceous unit of the Jebel Djedaria and show a moderate angular unconformity of about 15°. The  
282 Paleogene (Paleocene and Eocene) subhorizontal sequences of Lansarine consist of two units forming  
283 the so-called “Lansarine nappe” (Masrouhi et al., 2007). The previous mapping estimates a  
284 southeastward advance of about 10 km from the peel thrust of Mateur, themselves are displaced, which  
285 therefore constitutes a minimum estimation based on erosion limits. The thrust overlaps are well  
286 fossilized in the entire Lansarine plateau. The top of the Miocene sequences under the thrust was dated  
287 as Serrevalian. This implies that this configuration attests at least two tertiary compressional events. A  
288 first Eocene episode with a moderate folding which corresponds to the well-known Atlassic  
289 compressional event (Masrouhi et al., 2008) recognized on the overall scale of the Maghreb (Frizon de  
290 lamotte et al., 2000; Dhahri and Boukadi, 2010). A second paroxysmal Tortonian compression (the  
291 Alpine phase) is responsible for the present structure and deformations observed along this region  
292 (Chihi, 1992; Bouaziz et al., 2002; Bahrouni et al., 2014, Gharbi et al., 2014; Ahmadi et al., 2019).

293 The second characteristic, well identified by maps and geometric relationships between entities, is the  
294 E-trending fault systems. This Atlassic domain shows active N110-120° E-trending faults systems  
295 involved in the tertiary deformation affecting all sediments including the Mio-Pliocene sequences, which  
296 confirms their recent activity. This system frequently displays a multiphase striation for which the first  
297 one is classically related to the Mesozoic extensional period. This system is usually associated to  
298 thickness variations, slump folds and conglomeratic horizons indicative of their early Mesozoic  
299 evolution. Using the fault diagram, we rotated the collected fault data (Fig. 7) to restore the bedding  
300 plane to its horizontal orientation. We also used the back-tilting fault kinematics analysis of Naji et al.,  
301 (2018b) carried out in the northern Tunisian domain. The back-tilting result shows that these faults were  
302 normal faults predating the Cenozoic tilting (Fig. 7). Back-tilting of the measured lower Cretaceous fault  
303 population indicates a normal faulting that result from an extensional tectonic regime locally  
304 characterized by NE-SW minimum stress axis (Fig. 7). The back-tilting of the Aptian–Albian measured  
305 fault population indicates a normal faulting that result from an extensional tectonic regime locally

306 characterized by E-W to NE-SW minimum stress axis (Fig. 7). This phase is mainly characterized by NW-  
307 trending fault systems and associated sub-basins. This change from lower Cretaceous to Aptian-Albian  
308 periods, is interpreted in Tunisia as the translation from the Jurassic E-W (present-coordinates)  
309 dominant shape to Early Cretaceous NW-SE shape, which is concordant with the general E-W transform  
310 faults of the Atlantic that translate to NW-SE during the Alpine Tethys faults (Rosenbaum et al, 2002;  
311 Frizon de Lamotte et al., 2013; Masrouhi et al., 2019). The tectonic regime changes during the late  
312 Cretaceous post-Rift period. Locally, the Lansarine domain seems to be controlled by normal faults  
313 characterizing a NW-SE to N-S tectonic extension (Fig. 7).

#### 314 **4. Seismic interpretation**

315 Three seismic profiles are used and interpreted, for which some of them are composite ones. The  
316 seismic sections were provided by ETAP Petroleum National Company and the Carthago Oil Company  
317 Tunisia. For some section the acquisition was carried out by Shell-Tunirex Company in 1983. Seismic  
318 profile data are used to correlate the fault systems and/or tectonic blocks with the above-described  
319 sedimentary sequences. These Seismic profiles were correlated by petroleum wells as well as the  
320 stratigraphic sequences and outcrops established by the present-study fieldwork.

321 In this section, seismic profile interpretation is used to document the presence of allochthonous salt  
322 sheets and a buried salt diapir in the study area. Three seismic profiles are used to highlight the  
323 geometry at depth, halokinetic type and entities relationship. The seismic section L18 is a composite  
324 section derived along the Lansarine–Baouala region (Fig. 8). The ~ 35 km long NW-SE L18 profile crosses  
325 the LBSS near the Baouala structure (Fig. 3). Furthermore, two seismic profiles are used to highlight the  
326 distribution and the relationship between entities that are respectively the NE-SW L05 profile in the  
327 northern part and the NE-SW L11 profile in the southern part (with respect to the salt structure). These  
328 seismic profiles were analyzed and interpreted using calibration from the W-1, W-2 and W-3 petroleum  
329 wells (see Fig. 3 for location). The internal geometry of the shallow portion of the profiles in the LBSS is  
330 calibrated by the surface observations of this study.

331 The seismic section L18 highlights the Teboursouk and the Baouala fault zone that is characterized by a  
332 deep north-dipping basement fault and shallow listric normal faults within inferred Triassic evaporites,  
333 which confirms previous results (Rigo et al., 1996; Masrouhi et al., 2013). This basement fault zone was  
334 mostly active as a normal fault during Mesozoic times, allowing the deposition of a thick sedimentary  
335 pile in this northern Tunisian domain, reaching up to a thickness of 6 km. This major basement normal

336 faulting controls Mesozoic basin with associated changes in thickness well observed for the Jurassic and  
337 lower Cretaceous sequences. Structurally, it is clear that the present tectonic style of the area is the  
338 result of a post Cretaceous structural inversion. In this zone, the thick sedimentary cover is deformed by  
339 thrusts and large-scale folding above the southeastward major thrusts connected in the interface  
340 basement-cover (Triassic salt?). Thrusts are superimposed on deep seated basement faults which were  
341 active during Mesozoic times as major normal deep faults. The diapir, detected at depth for the first  
342 time, seems to be a minor complicating factor in Tertiary shortening deformations. Geometry, thickness  
343 variations, together with Triassic evaporites associated to a major thrust, suggest that the basement-  
344 cover interface geometry of this domain is poorly deformed (Fig. 8). The profile shows major thrust  
345 systems developed beneath the Chougui basin at the base of the basement–cover interface. The far  
346 northern part shows an imbrication of southeast-verging thrusts and gently dipping asymmetric folds  
347 filled by Oligocene-Miocene series (Fig. 8). The absence of the lower Cretaceous series in the hanging-  
348 wall and the base of these minor thrusts suggest a Cenozoic development. They probably do not  
349 correspond to inverted faults. In between, major southeast verging thrust systems are developed and  
350 major normal fault between Baouala block and Mateur plain are preserved. This seismic section  
351 underlines a buried diapir at depth. This stem of the LBSS is revealed as a salt body now buried under  
352 the complex thrust configuration of the LBSS. The main information highlighted by this seismic section is  
353 the compatibility between surface and subsurface data showing the presence of allochthonous salt  
354 sheets detected on the surface and their thinning towards the north. The salt sheet is detached from its  
355 autochthonous original position. A salt sheet (canopy?) is interlayered between lower Cretaceous beds.  
356 This 8 to-10 km-long salt sheet is actually located in the hanging-wall of the main southeastward thrust.  
357 The seismic section also highlights that salt tectonics seems to be controlled by Mesozoic normal  
358 faulting associated with well-developed rim synclines (salt mini-basins?) in lower Cretaceous thick  
359 sequences around the main salt body. Salt mini-basins are actually well recognized as being associated  
360 to salt movement in many worldwide salt provinces (Hudec and Jackson, 2007; Callot et al., 2012; callot  
361 et al., 2016). Mini-basins were likely formed as the result of the synsedimentary upward movement of  
362 Triassic salt conducted by the differential sedimentation loading itself guided by the major normal  
363 faulting. At present, the absence (or thinning?) of salt under Mateur plain may be explained by the  
364 lateral flow of salt from the main stem during Mesozoic times. This phenomenon, called salt evacuation,  
365 is well known in many other salt provinces (e.g. Gulf of Mexico, Santos basin ...).

366 The seismic section L05 crosses the northern domain and mainly shows an extensional geologic setting  
367 in this area (Fig. 9). This section was interpreted by Booth-Rea et al., (2018) as one of the low angle fault

368 systems named the Ghezala fault characterizing the extensional late Miocene collapse of northern  
369 Tunisia. This work interprets the major low angle normal faults as associated to high-angle faults  
370 producing a geometry characterized by half-graben and hanging-wall syncline basins during the late  
371 Miocene times. This interpretation of extensional collapse in the Atlas system during the late Cenozoic  
372 African-Eurasian convergence setting was related to deep mantle tectonic mechanisms in the  
373 concomitant extension of Tyrrhenian basin to East. While we agree with the core interpretation of  
374 Booth-Rea et al., (2018), we enhance and add some details in this section. The Miocene extensional  
375 system appears to be connected down on a major normal fault system (affecting both basement and  
376 cover, Fig. 9) such faults are probably inherited from the former Mesozoic Tethyan extensional period  
377 later reactivated during late Miocene times. This section highlights a lower Miocene extensional period.  
378 This extension, which occurred after the short Eocene compression, is mainly accommodated by large  
379 extensional faults connected down on basement faults systems that seem to be inherited from the  
380 former Tethyan basin.

381 The NE-SW seismic line L11 is located in the front of the thrust systems of LBSS and shows a narrow  
382 basin filled by Mio-Plio-Quaternary sediments reaching a 3 km of thickness (Fig. 10). In opposition to the  
383 northern domain, this section mainly exhibits high-angle normal fault systems. This narrow basin is  
384 mainly recorded by Miocene syntectonic strata. Regarding the position (between the Baouala thrust and  
385 the major Teboursouk thrust), the connected high angle normal faults and the sequences in this narrow  
386 basin are all interpreted as an orthogonal extension in which the thrust strongly influences the  
387 development of normal faults. This section exhibits a strong variation in thickness associated to faults. In  
388 addition, the thickness variations are remarkable for Jurassic and lower Cretaceous sequences, which  
389 testifies that this fault is inherited from Mesozoic times.

390 The seismic data seems to be well correlated with gravity results recently presented by Sarsar et al.  
391 (2017). According to the superimposition of the Euler solutions to Bouguer Anomaly map used to  
392 present the distribution of anomalies and curved gravity lineaments about positive anomalies and also  
393 estimate the depth of those anomalies, Sarsar et al. (2017) suggest that the west of the LBSS  
394 corresponds to a fault concentric zone and provides the evidence of a pre-existing diapiric geometry  
395 body located at the depth between 1 and 2 Km and later buried by Mesozoic and Cenozoic sediments.  
396 The NW-trending of the main gravity contours reach a depth of 2 km and confirm the existence of the  
397 Teboursouk fault as a major thrust fault system. This system is probably inherited from Mesozoic times  
398 and acted as the main control in favor of diapir upward (for more details see Sarsar et al., 2017). The

399 concentric behavior in the west of the LBSS is probably connected downward to the Teboursouk thrust,  
400 which explains the presence of sub-Triassic structures in this belt.

## 401 5. Discussion

402 *i. Previous interpretations:* Several interpretations were made separately by several authors to  
403 explain the diapiric structure that may be summarized as follows: 1- Bolze (1954) suggests a salt move-  
404 up because of space creation via normal faulting, 2- Zargouni (1975) suggests a scenario in which salt  
405 intrudes forcefully into its overburden during Mesozoic and Eocene times, and 3- Perthuisot (1978)  
406 suggests a way in which salt intruded forcefully into its overburden during late Cretaceous-Eocene  
407 compression. This structure, called by all previous studies "the Lansarine diapir », was presented as a  
408 cylindrical, 45 km long and 15 km-wide vertical diapir. Our field mapping does not support this  
409 hypothesis of a single 15 km-wide vertical diapir. The structure and the salt budget do not permit to  
410 interpret it as one rooted salt structure. 4- Truillet and Deltail (1982) propose a large thrusting system.  
411 Based on the observation that the Triassic salt is interbedded and subparallel to the Cretaceous layers,  
412 this work propose that all this region corresponds to a large tectonic nappe and must be integrated to  
413 the front of the Numidian allochthonous zone. 5- Finally Masrouhi et al. (2013) propose a salt canopy  
414 model. This model proposes a scenario in which extension induces normal faults that provide routes to  
415 the salt to reach the surface and flow downslope.

416 *ii. Field data discussion and tectono-sedimentary features:* Field work, together with the  
417 interpretation of seismic profiles, shows that the present LBSS may result from a long-time polyphasic  
418 geological history. This 45 km-long and 15 to 5 km-wide salt structure was likely passively transported on  
419 major thrusts during the Atlasic and Alpine shortening. These main tectonics events are recognized to  
420 occur during the Late Eocene (Atlastic) and Miocene–to present-day for the alpine event (e.g. El Ghali et  
421 al., 2003; Masrouhi et al., 2008; Dhahri and Boukadi, 2010). The present structure is also the result of  
422 considerable erosion and probably dissolution during late Cretaceous and Cenozoic times. It likely  
423 covered a wider area during Mesozoic times. In this study we confirm by seismic examination the  
424 presence of a salt diapir body deeply buried under a complex thrust system which was absent in the  
425 previous interpretation. We also confirm by surface data that the outlines of the Triassic salt are  
426 commonly subparallel to the bedding of the adjoining rocks succession of the northern and southern  
427 parts. The contacts of the Triassic rocks are not discordant with them. Geologic map and field cross  
428 sections are consistent with an allochthonous sheet of Triassic salt emplaced over the Early Cretaceous  
429 successions. For the LBSS, field data emphasizes the absence of radial faulting that is usually associated



430 with diapirism growth well observed and documented in others salt province (e.g. Rowan et al., 2003;  
431 Yin et al., 2009). Based on field investigations, we therefore suggest (for the central and northern part) a  
432 composite salt sheet covering Early Cretaceous sediments. Established by seismic interpretation, a  
433 diapiric stem is detected under the LBSS large salt sheet. In the LBSS area, Early Cretaceous sediments  
434 are characterized by considerable variation in thickness and exhibit numerous sedimentary features  
435 (nodules reworking, slumps and conglomerates lenses) within an active extensional tectonic regime  
436 (Naji et al., 2018b). This created an irregular seafloor resulting from normal faulting. In the LBSS area,  
437 several preserved extensional structures as small-scale sealed normal faults constitute a useful marker  
438 for this tectonic activity. Structurally, the LBSS structure occupies a position in the intersection of the  
439 major faults systems i.e., the E-trending strike-slip and the NE-trending thrusts fault systems. Surface  
440 data together with the seismic profile interpretation highlight a general shallow north-dipping high-  
441 angle normal fault above a major deep listric one. Mechanically, this can explain the weakened  
442 overburden of the Triassic salt. The LBSS corresponds at present to a complex structure involving Triassic  
443 salt and bounded by north dipping fault systems (Figs. 7-10). It seems to be the stem of the LBSS diapir  
444 during Mesozoic time before the Atlasic shortening. This emplacement was likely driven by normal  
445 faulting, which affected both the cover and the basement, along with differential loading. This context  
446 fits with the southern Tethyan passive margin setting well documented by previous studies (e.g.  
447 Souquet et al., 1997; Jaillard et al., 2013; Soua, 2014; El Amari et al., 2016; Naji et al., 2018a).

448 **iii. Diapirism style:** Taking in account the overall structure, the LBSS shows strong similarities to  
449 those recently described by authors around many salt provinces (e.g. Saura et al., 2014; Alsop et al.,  
450 2015; Martin-Martin et al., 2017; Jaillard et al., 2017; Zucker et al., 2019). The halokinesis process was  
451 particularly active during the rifting stage, in which tilted block geometry was responsible for differential  
452 loading. During the Alpine compression, diapiric salt corresponds to weak surfaces used by the Alpine  
453 thrust systems. Structural analysis indicates that the LBSS emplacement was guided by a basement  
454 normal fault system related to the south Tethyan rifting. The general framework of this margin, together  
455 with similarities between the LBSS and recently published diapirs from other salt provinces, led to the  
456 proposal of polyphase diapirism history. Within the Maghreb framework (e.g. Soussi et al., 2017; Dhahri  
457 and Boukadi, 2017; Ahmadi et al., 2019), the Jurassic–Early Cretaceous extensional context of the south  
458 Tethyan margin in Tunisia allows a reactive mobilization of salt layers. This tectonic setting offers two  
459 conditions allowing salt to extrude onto the sea-floor. (1) The extension weakens the overburden by  
460 normal faulting creating space for salt to rise forming the diapir structure and (2) induces thickness  
461 variations leading to differential loading which initiate the salt movement (Fig. 11). During the Tethyan

462 rifting period, lower Cretaceous extensional tectonic regime induced thick depositional basin sediments  
463 controlled by major basement normal faults. Within this structural setting, well recorded in North  
464 Tunisia, the salt's overburden was weakened by faulting creating space, along with salt (acknowledged  
465 to be Newtonian fluid at depth) withdrawing from the weakened zone by faulting. Accumulation of thick  
466 salt overburden in subsiding area acts as a rapid differential loading that encourages salt flow from the  
467 diapir stem. This evolution corresponds to a reactive diapir (sensu Vendeville and Jackson, 1992b), which  
468 extruded along the main fault system (Fig. 11). Active diapirism would correspond to a short lower  
469 Cretaceous event, currently not observable because it has been overprinted by tectonic compressional  
470 deformations. The basement fault movement, salt withdrawal and growth of diapir itself; all of them  
471 may have induced a significant asymmetry creating salt mini-basins well recognized as associated to salt  
472 movement in many worldwide salt provinces. Above-mentioned observations indicate a structural  
473 configuration that led to lateral spreading onto the depositional surface over the LBSS diapiric stem (Fig.  
474 11). It corresponds to a well-known salt process that could be active both in submarine (Fletcher et al.,  
475 1995) and sub-aerial environments (Talbot, 1998).

476 **iv. Regional consideration:** The structural style of the LBSS seems to be very similar to other  
477 structures recognized as being the result of basement faults movement, on which extensional thin-  
478 skinned deformation is connected. The trigger mechanism of salt migration of the LBSS can be compared  
479 to other similar salt provinces: e.g., Pyrenean orogen (Canérot et al., 2005; Saura et al., 2016), the  
480 Eastern Betics (Roca et al., 2013; Rubinat et al., 2013), Nordkapp Basin (Koyi et al., 1995), or North Africa  
481 (Bouchouata et al., 1995; Saura et al., 2013, Masrouhi et al., 2014a, Moragas et al., 2017, 2019). The  
482 original criteria of the Salt structure is preserved likely because it was passively transported on major  
483 thrusts, superimposed on deep seated basement faults, during the Atlassic and Alpine shortening  
484 periods. The Northeastern Maghreb domain is one of the world's least-known areas in terms of salt  
485 tectonics (Hudec and Jackson, 2007). It appears similar to many others inverted salt provinces, for which  
486 it is difficult to interpret the original geometry and evolution of salt diapirs. In this domain, the  
487 buoyancy-driven halokinetic model has long been considered as the unique way of salt growth. This  
488 model postulated an autonomous isostatic rise of salt and piercement of the overburden due to the  
489 Rayleigh–Taylor instabilities. Based on this model, the diapirs of North Tunisia have been considered to  
490 expose only “vertical” diapir structures (Perthuisot, 1978; Perthuisot et al., 1998; Rouvier et al., 1998;  
491 Jallouli et al., 2005). Recently, an allochthonous salt model has been documented by Masrouhi et al.  
492 (2013) in the Alpine thrust front of Teboursouk (Teboursouk thrust unit, Fig. 1). The authors suggest a

493 scenario where salt broke out at the sediment–water interface or below a thin layer of marine  
494 sediments forming an allochthonous extrusion, similar to the present-day salt tectonics described in the  
495 deep–water Gulf of Mexico (Fletcher et al., 1995) or Angola margin (Fort et al., 2004; Ge et al., 2019).  
496 Later, the pre-existing allochthonous salt was deformed during Miocene–present day Alpine  
497 compressions that used the weakness of the salt sheet as thrust décollement. The interconnection  
498 between these two types (i.e. vertical diapir and large connected salt sheet) has never been described  
499 yet.

500 **v. The LBSS style:** The LBSS clearly shows asymmetric overhangs flowing northward (the subsiding  
501 area). The first part of the LBSS evolution for the sheet connected to the Lansarine salt diapir can be  
502 easily distinguished as an extrusive advance (*sensu* Hudec and Jackson, 2006), in which an exposed salt  
503 sheet spreads at the water–sediment interface without any roof. Above the apex of the diapir, that  
504 corresponds to the feeder, salt flows outward and spreads by gravity downslope (Fig. 11). The  
505 overburden on the salt may have formed a synclinal minibasin on top of the salt sheet (Fig. 11). In this  
506 case, the minibasin had a thickness usually determined by the salt evacuation budget forming in some  
507 cases a salt weld (e.g. Diegel et al., 1995; Schuster, 1995; Callot et al., 2012). In this domain, the low-  
508 amplitude syncline of Chouigui (Fig. 9) is likely the minibasin developed by evacuation of allochthonous  
509 Triassic salt during Mesozoic times (see Fig. 11). From late Cretaceous to Eocene time, the onset of the  
510 compressional Atlassic stage (e.g. Guiraud and Bosworth, 1997; Frizon de Lamotte et al., 2000) resulted  
511 in widespread shortening associated with the inversion of the normal faults and probably without  
512 significantly compressing the LBSS. The diapir was passively transported above the southeast-verging  
513 major thrust which is deeply rooted in the salt beneath the Mateur plain (Fig. 11). During this period, the  
514 LBSS was eroded due to fold-related uplifting.

515

## 516 **6. Conclusion**

517 Based on the results of detailed field work and seismic profiles' interpretation of the Lansarine-Baouala  
518 Salt Structure in the Northern Atlassic domain of Tunisia, the following conclusions can be made:

- 519 • Salt diapirism in Northern Tunisia appears to be contemporaneous with tectonic extension. The  
520 Jurassic–Early Cretaceous extensional tectonic context of the southern Tethyan margin induced  
521 thick depositional basin sediments controlled by major basement normal faults. The extension

522 weakens the overburden by normal faulting and the thickness variations leading to differential  
523 loading which allow a reactive mobilization of Triassic evaporites,

524 • During Mesozoic diapirism phase, a significant allochthonous salt spreads laterally from the diapir  
525 stem. Salt flows outward and spreads by gravity downslope highlighting an extrusive sheet  
526 advance. In this domain, the low-amplitude syncline of Chouigui seems to be a minibasin  
527 developed in conjunction with the evacuation of allochthonous Triassic salt during Mesozoic  
528 times,

529 • Compressional deformation stages do not reflect active diapirism. The Lansarine diapir and its  
530 connected salt sheet were passively transported on the southeast-verging major thrust deeply  
531 rooted in the salt beneath the Mateur plain during the Atlassic and Alpine shortening. In the north  
532 Tunisian domain, the identification of allochthonous Triassic salt sheets connected to buried  
533 diapir have a significant role in the shallow structural complexity observed in the sedimentary  
534 cover during the subsequent contractional events.

535

### 536 **Acknowledgments**

537 This work was financially supported by the Tunisian Ministry of Higher Education and Scientific Research  
538 (CERTE, Geo-resources Laboratory funding) and the French Ministry of Foreign Affairs grant through  
539 French Embassy in Tunisia (CMCU program). This work is a contribution to the program of the French  
540 National Research Agency (ANR) through the A\*MIDEX OT-Med project (nANR-11-LABX-0061) funded by  
541 the French Government «Investissements d'Avenir» (n ANR-11-IDEX-0001-02). We are grateful to Franck  
542 Thomas for providing constructive help that substantially improved the structure of this paper. Authors  
543 are thankful to the Editor Mohamed G Abdelsalam as well as the reviewers for their constructive  
544 suggestions and comments.

545

546 **References**

- 547 Ahmadi, R., Mercier, E., Trigui, H., Abdennaceur Ouali, J., 2019. Relationship between fractures patterns  
 548 and fold kinematics; the case study of Jebel Sehib, a typical fault propagation fold of southern Tunisia,  
 549 *Journal of African Earth Sciences*, 125, 23-35.
- 550 Allen, J., Beaumont, C., Deptuck, M. E., 2020. Feedback between synrift lithospheric extension,  
 551 sedimentation and salt tectonics on wide, weak continental margins. *Petroleum Geoscience*, 26 1, 16–  
 552 35.
- 553 Allen, P. A., Allen, J. R., 1990. *Basins analysis: Principles and Applications*, 2d: New York, Wiley–Backwell,  
 554 560 p.
- 555 Alouani, R., Melki F., Tlig, S., Zargouni, F. 2006. Geologic map of Menzel Bourguiba 1:50000, sheet n°6.  
 556 National Geological Survey. National Office of Mines, Tunisia.
- 557 Alsop, G. I., Marco, S., 2014. Fold and fabric relationships in temporally and spatially evolving slump  
 558 systems: A multi-cell flow model. *Journal of Structural Geology*, 63, 27–49.
- 559 Alsop, G. I., Weinberger, R., Levi, T., Marco, S., 2015. Deformation within an exposed salt wall:  
 560 Recumbent folding and extrusion of evaporites in the Dead Sea Basin. *Journal of Structural Geology* 70,  
 561 95-118.
- 562 Bahrouni, N., Bouaziz, S., Soumaya, A., Ben Ayed, N., Attafi, K., Houla, Y., El Ghali, A., Rebai, N., 2014.  
 563 Neotectonic and seismotectonic investigation of seismically active regions in Tunisia: A multidisciplinary  
 564 approach. *Journal of Seismology*, 18, 2, 235-256.
- 565 Bally, A.W., 1983. Seismic expression of structural styles. *AAPG Studies in Geology*, 15, 3, 29 p.
- 566 Ben Ferjani, A., Burolet, P.F., Mejri, F., 1990. *Petroleum geology of Tunisia*, ETAP Memoir eds, 194 p.
- 567 Benaouali-Mebarek, N., Frizon de Lamotte, D., Roca, E., Bracène, R., Faure, J. L., Sassi, W., Roure, F.,  
 568 2006. Post-Cretaceous kinematics of the Atlas and Tell systems in central Algeria: Early foreland folding  
 569 and subduction-related deformation, *C. R. Geosci.*, 338, 115-125.
- 570 Benassi, R., Jallouli, Ch., Hammami, M., Turki, M. M., 2006. The structure of Jebel El Mourra, Tunisia: a  
 571 diapiric structure causing a positive gravity anomaly. *Terra Nova*, 18, 432-439.
- 572 Billi, A., Faccenna, C., Bellier, O., Minelli, L., Neri, G., Piromallo, C., Presti, D., Scrocca, D., Serpelloni, E.,  
 573 2011. Recent tectonic reorganization of the Nubia–Eurasia convergent boundary heading for the closure  
 574 of the western Mediterranean. *Bull. Soc. Geol. Fr*, 182, 279-303.
- 575 Bolze, J., 1950. Diapirs triasiques et phases orogéniques dans les monts de Téboursouk (Tunisie  
 576 septentrionale). *C. R. Acad. Sci. Paris*, t 231, n° 8, 480-482.
- 577 Bolze, J., 1954. Ascension et percée des diapirs au Crétacé moyen dans les monts de Téboursouk  
 578 (Tunisie septentrionale). *C. R. Somm. Soc. Géol. France*, 139-141.
- 579 Booth-Rea, G., Gaidi, S., Melki, F., Marzougui, W., Azañón, J. M., Zargouni, F., Galvé, J. P., Pérez-Peña, J.  
 580 V. 2018a. Late Miocene Extensional Collapse of Northern Tunisia, *Tectonics*, 37, 1626- 1647.
- 581 Bouaziz, S., Barrier, E., Soussi, M. M., Turki, M.M., Zouari, H., 2002. Tectonic evolution of the northern  
 582 African margin in Tunisia from paleostress data and sedimentary record. *Tectonophysics*, 357, 227-253.
- 583 Bouchouata, A., Canerot, J., souhel, A., Almeras, Y., 1995. Stratigraphie séquentielle et évolution  
 584 géodynamique du jurassique dans la région de Talmest-Tazoult (Haut Atlas central, Maroc), *C.R. Acad.*  
 585 *Sci. Paris*, 320, 749-756.

- 586 Boughdiri, M., Cordey, F., Sallouhi, H., Maalaoui, K., Masrouhi, A., Soussi, M., 2007. Jurassic radiolarian-  
587 bearing series of Tunisia: biostratigraphy and significance to western Tethys correlations. *Swiss J. Geosci.*,  
588 100, 431-441.
- 589 Brune, S., Heine, C., Perez-Gussinye, M., and Sobolev, S., V., 2014: Rift migration explains continental  
590 margin asymmetry and crustal hyper-extension, *Nat. Commun.*, 5. Ncomms 5014, 2014.
- 591 Burollet, P.F., 1956. Contribution à l'étude stratigraphique de la Tunisie centrale. *Annales des Mines et*  
592 *de la Géologie (Tunisie)*, vol. 18, 350 p.
- 593 Callot, J.P., Ribes, C., Kergaravat, C., Bonnel, C., Temiz, H., Poisson, A., Vrielynck, B., Ringenbach, J.C.,  
594 2014. Salt tectonics in the Sivas Basin (Turkey), Walking across salt wall and minibasins. *Bull. Soc. Geol.*  
595 *France*, 185, 1.
- 596 Callot, J.P., Salel, J.F., Letouzey, J., Daniel, J.M., Ringenbach, J.C., 2016. Three dimensional evolution of  
597 salt-controlled minibasins: Interactions, folding, and megafault development. *AAPG Bulletin* 100 (9):  
598 1419-1442.
- 599 Callot, J.P., Trocmé, V., Letouzey, J., Albouyi, E., S. Jahani, S. Sherhati., 2012. Pre-existing salt structures  
600 and the folding of the Zagros Mountain. *Geological Society, London, Special Publications*, 363, 545–561.
- 601 Canérot, J., Hudec, M.R., Rockenbauch, K., 2005. Mesozoic diapirism in the Pyrenean orogen: salt  
602 tectonics on a transform plate boundary. *American Association of Petroleum Geologists Bulletin* 89, 211-  
603 229.
- 604 Chihi, L., 1992. Seismotectonic study in Central and Southern Tunisia. *Tectonophysics*, 209, 1-4, 175-178.
- 605 Cordey, F., Boughdiri, M., Sallouhi, H., 2005: First direct age determination from the Jurassic radiolarian-  
606 bearing siliceous series (Jéjidi Formation) of northwestern Tunisia. *Comptes Rendus Geoscience Paris*  
607 337, 777-785.
- 608 Deverchere, J., Yelles, K., Domzig, A., De Lepinay, M., B., Bouillin, J. P., Gaullier, V., Bracene, R., Calais, E.,  
609 Savoye, B., Kherroubi, A., Le Roy, P., Pauc, H., Dan, G., 2005. Active thrust faulting offshore Boumerdes,  
610 Algeria, and its relations to the 2003 Mw 6.9 earthquake. *Geophys. Res. Letters*, 32, L04311.
- 611 Dhahri, F., Boukadi, N., 2010. The evolution of pre-existing structures during the tectonic inversion  
612 process of the Atlas chain of Tunisia. *Journal of African Earth Sciences*, 56, 139–149.
- 613 Dhahri, F., Boukadi, N., 2017. Triassic salt sheets of Mezzouna, central Tunisia: new comments on Late  
614 Cretaceous halokinesis and geodynamic evolution of the Northern African margin. *Journal of African*  
615 *Earth Sciences*, 129, 318-329.
- 616 Diegel, F. A., Karlo, J.F. Schuster, D.C. Shoup, R. C., Tauvers, P. R., 1995. Cenozoic structural evolution  
617 and tectonostratigraphic framework of the northern Gulf Coast continental margin, In *Salt tectonics: A*  
618 *global perspective* (eds. Jackson, M. P. A. Roberts, D. G., Snelson, S.) *American Association of Petroleum*  
619 *Geologists Memoir*, 65, 109-151.
- 620 Dlala, M., 1992. Seismotectonic study in Northern Tunisia. *Tectonophysics*, 209, 1-4, 171-174.
- 621 Dlala, M., Hfaiedh, M., 1993. Le séisme du 7 novembre 1989 à Metlaoui (Tunisie méridionale): une  
622 tectonique active en compression. *C. R. Acad. Sci. Paris Série II*, 317, 10, 1297-1302.
- 623 Dooly, T.P., Hudec, M.R., Pichel, L.M., Jackson, M.P.A., 2018. The impact of base-salt relief on salt flow  
624 and suprasalt deformation patterns at the autochthonous, paraautochthonous and allochthonous level:  
625 insights from physical models. In *Mc Clay, K. R. & Hammerstein, J. A. (eds) Passive Margins: Tectonics,*  
626 *Sedimentation and Magmatism. Geological Society, London, Special Publications*, 476.

- 627 El Amari, E.A., Gharbi, M., Youssef, M.B., Masrouhi, A., 2016. The structural style of the southern Atlasic  
628 foreland in northern Chotts range in Tunisia: field data from Bir Oum Ali structure. *Arab. J. Geosci.* 9,  
629 389.
- 630 El Ghali, A., Ben Ayed, N., Bobier, C., Zargouni, F., Krifa, A., 2003. Les manifestations tectoniques  
631 synsédimentaires associées à la compression éocène en Tunisie, implications paléogéographiques et  
632 structurales sur la marge Nord-Africaine, *C. R. Geoscience* 335, 763-771.
- 633 Espurt, N., Angrand, P., Teixell, A., Labaume, P., Ford, M., De Saint Blanquat, M., Chevrot, S., 2019.  
634 Crustal-scale balanced cross-section and restorations of the Central Pyrenean belt (Nestes-Cinca  
635 transect): Highlighting the structural control of Variscan belt and Permian-Mesozoic rift systems on  
636 mountain building. *Tectonophysics*, 764, 25-45.
- 637 Fernandez, N., Hudec, M.R., Jackson, C.A.L., Dooley, T.P., Duffy, O.B., 2020. The competition for salt and  
638 kinematic interactions between minibasins during density-driven subsidence: observations from  
639 numerical models. *Petroleum Geoscience*, 26, 1, 3–15.
- 640 Fletcher, R.C., Hudec, M. R., Watson, I. A. 1995. Salt glacier and composite sediment: salt glacier models  
641 for the emplacement and early burial of allochthonous salt sheets. In *Salt Tectonics: A Global  
642 Perspective* (eds. Jackson, M. P. A. Roberts, D. G., Snelson, S.). American Association of Petroleum  
643 Geologists Memoir, 65, 77-108.
- 644 Fort, X., Brun, J.P., 2004. Compressional salt tectonics (Angolan Margin). *Tectonophysics*, 382(3) : 129-  
645 150.
- 646 Fort, X., Brun, J.P., Chauvel, F., 2004. Salt tectonics on the Angolan margin, synsedimentary deformation  
647 processes. *Bulletin of the American Association of Petroleum Geologists*, 88, 1523-1544.
- 648 Frizon de Lamotte, D., Leturmy, P., Missenard, Y., Khomsi, S., Ruiz, G., Saddiqi, O., Guillocheau, F.,  
649 Michard, A., 2009. Mesozoic and Cenozoic vertical movements in the Atlas system (Algeria, Morocco,  
650 Tunisia): an overview. *Tectonophysics*, 475, 9-28.
- 651 Frizon de Lamotte, D., Raulin, C., Mouchot, N., Wrobel-Daveau, J.C., Blanpied, C., Ringenbach, J.C., 2013.  
652 The southernmost margin of the Tethys Realm during the Mesozoic and Cenozoic: Initial geometry and  
653 timing of the inversion processes. *Tectonics*, 30, TC3002, 1-22.
- 654 Frizon de Lamotte, D., Saint-Bezar, B., Bracene, R., Mercier, E., 2000. The two main steps of the Atlas  
655 building and geodynamics of the western Mediterranean. *Tectonics*, 19, 740-761.
- 656 Ge Z, Gawthorpe, R.L., Rotevatn, A., Zijerveld, L., Jackson, A.L.C., Oluboyo, A., 2019. Minibasin  
657 depocentre migration during diachronous salt welding, offshore Angola. *Basin Res.* 2019, 00, 1–19.
- 658 Ghanmi, M., Ben Youssef, M., Jouirou, M., Zargouni, F., Vila J. M., 2001. Halocinèse crétacée au Jebel  
659 Kebbouch (Nord-Ouest tunisien) : mise en place à fleur d'eau et évolution d'un « glacier de sel » albien,  
660 comparaisons. *Eclogae Geologicae Helvetiae*, 94, 153-160.
- 661 Gharbi, M., Bellier, O., Masrouhi, A., Espurt, N., 2014. Recent spatial and temporal changes in the stress  
662 regime along the southern Tunisian Atlas front and the Gulf of Gabes: New insights from fault  
663 kinematics analysis and seismic profiles. *Tectonophysics*, 626, 120-136.
- 664 Gharbi, M., Espurt, N., Masrouhi, A., Bellier, O., Amari, E.A. 2015. Style of Atlasic tectonic deformation  
665 and geodynamic evolution of the southern Tethyan margin, Tunisia. *Marine and Petroleum Geology*, 66,  
666 801-816.
- 667 Giles, K. A., Rowan, M. G., 2012. Concepts in halokinetic-sequence deformation and stratigraphy. In G. I.  
668 Alsop, S. G. Archer, A. J. Hartley, N. T. Grant, R. Hodgkinson (Eds.), *Geological Society of London Special*

- 669 Publications: Vol. 363. Salt tectonics, sedimentation and prospectivity (pp. 7–31). London: The  
670 Geological Society.
- 671 Guiraud, R., Bosworth, W., 1997. Senonian basin inversion and rejuvenation of rifting in Africa and  
672 Arabia: synthesis and implications to plate-scale tectonics. *Tectonophysics*, 282, 39-82.
- 673 Hearon IV, T. E., Rowan, M. G., Giles, K. A., Kernan, R. A., Gannaway, C. E., Lawton, T. F., Fiduk, J. C.,  
674 2015. Allochthonous salt initiation and advance in the northern Flinders and eastern Willouran ranges,  
675 South Australia: Using outcrops to test subsurface-based models from the northern Gulf of Mexico.  
676 *AAPG Bulletin*, 99, 293–331.
- 677 Heydarzadeh, K., Ruh, J. P., Vergés, J., Hajjalibeigi, H., Gharabeigli, G., 2020. Evolution of a structural  
678 basin: Numerical modelling applied to the Dehdasht Basin, Central Zagros, Iran. *Journal of Asian Earth  
679 Sciences*. 187 (2020) 104088.
- 680 Hudec, M.R., Jackson, M.P.A., 2004. Regional restoration across the Kwanza Basin, Angola: salt tectonics  
681 triggered by repeated uplift of a metastable passive margin. *American Association of Petroleum  
682 Geologists Bulletin*, 88, 971-990.
- 683 Hudec, M.R., Jackson, M.P.A., 2006. Advance of allochthonous salt sheets in passive margins and  
684 orogens. *American Association of Petroleum Geologists Bulletin*, 90, 1535-1564.
- 685 Hudec, M.R., Jackson, M.P.A., 2007. Terra infirma: understanding salt tectonics. *Earth Science Reviews*  
686 82, 1-28.
- 687 Hudec, M.R., Jackson, M.P.A., 2009. Interaction between spreading salt canopies and their peripheral  
688 thrust systems. *Journal of structural geology*, 31, 1114-1129.
- 689 Jackson, M., Hudec, M. (2017). Salt Sheets and Salt Canopies. In *Salt Tectonics: Principles and Practice*,  
690 119–154. Cambridge: Cambridge University Press. Doi:10.1017/9781139003988.009.
- 691 Jackson, M.P.A., Talbot, C.J., 1989. Anatomy of mushroom-shaped diapirs, *Journal of structural geology*,  
692 11, 211-230
- 693 Jackson, M.P.A., Vendeville, B.C., 1994. Regional extension as a geologic trigger for diapirism. *GSA  
694 Bulletin*, 106, 57-73.
- 695 Jaillard, E., Bouillin, J. P., Ouali, J., Dumont, T., Latil, J. L., Chihaoui, A., 2017. Albian salt-tectonics in  
696 Central Tunisia: Evidences for an Atlantic-type passive margin. *Journal of African Earth Sciences*, 135,  
697 220-234.
- 698 Jaillard, E., Dumont, T., Ouali, J., Bouillin, J. P., Chihaoui, A., Latil, J. L., Arnaud, H., Arnaud-Vanneau, A.,  
699 Zghal, I., 2013. The Albian tectonic “crisis ”in Central Tunisia: Nature and chronology of the  
700 deformations. *Journal of African Earth Sciences*, 85, 75-86
- 701 Jallouli, C., Chikhaoui, M., Brahem, A., Turki, M. M., Mickus, K., Benassi R., 2005. Evidence for Triassic  
702 salt domes in the Tunisian Atlas from gravity and geological data. *Tectonophysics*, 396, 209-225.
- 703 Jauzein, A., 1962. Contribution à l'étude géologique de la Tunisie septentrionale : les confins de la  
704 dorsale tunisienne (zone des dômes et sahels). Thèse Paris, *Annales des Mines et de la géologie*. Tunis  
705 n°22.
- 706 Jolivet, L., Faccenna, C., 2000. Mediterranean extension and the Africa-Eurasia collision. *Tectonics*,  
707 2000TC900018.
- 708 Kergaravat, C., Ribes, C., Legeay E., Callot, J.-P., Kavak, K. S., Ringenbach, J.-C., 2016. Minibasins and salt  
709 canopy in foreland fold-and-thrust belts: The central Sivas Basin, Turkey, *Tectonics*, 35, 1342–1366.



- 710 Khessibi, M., 1967. Etude stratigraphique et structurale des formations mésozoïques de Djédeida-  
711 beauvoir (Tunisie). Dipl. Et. Sup. Univ. Tunis. 80 p. (déposé au Service Géologique de Tunisie).
- 712 Koyi, H., Talbot, C., Tørudbakken, B. 1995, salt tectonics in Northeastern nordkapp basin, Southwestern  
713 Barents Sea, In Salt tectonics: A global perspective (eds. Jackson, M. P. A. Roberts, D. G., Snelson, S.) pp.  
714 437-447. American Association of Petroleum Geologists Memoir no. 65.
- 715 Laaridhi-Ouazaa, N., 1994. Etude minéralogique et géochimique des épisodes magmatiques  
716 mésozoïques et miocènes de la Tunisie. Thèse Doc. Etat, University Tunis II, Tunisia, 466 p.
- 717 Martin-Martin, J.D., Vergés, J., Saura, E., Moragas, M., Messenger, G., Baqués, V., Razin, P., Grélaud, C.,  
718 Malaval, M., Joussiaume, R., Casciello, E., Cruz-Orosa, I., Hunt, D.W., 2017. Diapiric growth within an  
719 Early Jurassic rift basin: The Tazoult salt wall (central High Atlas, Morocco). *Tectonics*, 36, 1, 2-32.
- 720 Masrouhi, A., 2006. Les appareils salifères des régions de Mateur, Tébourba et de Medjez-el-Bab  
721 (Tunisie du Nord). PhD thesis, department of Geology.Tunis-el-Manar University, 258 p, Published thesis.
- 722 Masrouhi, A., Bellier, O., Koyi, H., 2014b. Geometry and structural evolution of Lorbeus diapir,  
723 northwestern Tunisia: polyphase diapirism of the North African inverted passive margin. *Int J Earth Sci*  
724 *(Geol Rundsch)*, 103, 881-900.
- 725 Masrouhi, A., Bellier, O., Koyi, H., Vila, J. M., Ghanmi, M., 2013. The evolution of Lansarine-Baouala salt  
726 canopy in North African Cretaceous passive margin in Tunisia. *Geological Magazine*, 150 (5), 835-861.
- 727 Masrouhi, A., Bellier, O., Youssef, M.B., Koyi, H., 2014a. Submarine allochthonous salt sheets: gravity-  
728 driven deformation of North African Cretaceous passive margin in Tunisia e Bled Dogra case study and  
729 nearby salt structures. *Journal of African Earth Sciences*, 97, 125-142.
- 730 Masrouhi, A., Ghanmi, M., Ben Slama, M.M., Ben Youssef, M., Vila, J. M, Zargouni, F., 2008. New  
731 tectono-sedimentary evidence constraining the timing of the positive tectonic inversion and the Eocene  
732 Atlasic phase in northern Tunisia: Implication for the North African paleo-margin evolution. *C. R.*  
733 *Geosciences*, 340, 771-778.
- 734 Masrouhi, A., Ghanmi, M., Ben Youssef, M., Vila, J. M, Zargouni, F., 2007. Definition of a thrust nappe  
735 with two Palaeogene units in the Lansarine plateau (northern Tunisia): A new structural element of the  
736 Tunisian Atlas and reevaluation of the Tertiary compression phases. *C. R. Geosciences*, 339, 441-448.
- 737 Masrouhi, A., Gharbi, M., Bellier, O., Ben Youssef, M., 2019. The Southern Atlas Front in Tunisia and its  
738 foreland basin: Structural style and regional-scale deformation. *Tectonophysics*, 764, 1-24.
- 739 Masrouhi, A., Koyi, H., 2012. Submarine "salt glacier" kinematics of Northern Tunisia, a case of Triassic  
740 salt mobility in North African Cretaceous passive margin. In: Alsop, G.I., Archer, S.G., Hartley, A., Grant,  
741 N.T., Hodgkinson, R. (Eds.), *J. Geol. R. Salt Tectonics, Sediments and Prospectivity*. Geological Society,  
742 London, Special Publications, 363, 579-593.
- 743 Mattoussi Kort, H., Gasquet, D., Ikenne, M., Laridhi Ouazaa, N., 2009. Cretaceous crustal thinning in  
744 North Africa: Implications for magmatic and thermal events in the Eastern Tunisian margin and the  
745 Pelagic Sea. *Journal of African Earth Sciences*, 55, 5, 257-264.
- 746 Melki, F., Zouaghi, T., Harrab, S., Casas Sainz, A., Bédir, M., Zargouni, F., 2011. Structuring and evolution  
747 of Neogene transcurrent basins in the Tellian foreland domain, North-Eastern Tunisia. *Journal of*  
748 *Geodynamics*, 52, 57-69.

- 749 Moragas, M., Baqués, V., Travé, A., Martín-Martín, J.D., Saura, E., Messenger, G., Hunt, D., Vergés, J. 2019.  
750 Diagenetic evolution of lower Jurassic platform carbonates flanking the Tazoult salt wall (Central High  
751 Atlas, Morocco). Basin Research. In Press.
- 752 Moragas, M., Vergés, J., Nalpas, T., Saura, E., Martín-Martín, J.D., Messenger, G., Hunt, D.W., 2017. The  
753 impact of syn- and post-extension prograding sedimentation on the development of salt-related rift  
754 basins and their inversion: Clues from analogue modeling. Marine and Petroleum Geology 88, 985-1003.
- 755 Moragas, M., Vergés, J., Saura, E., Martín-Martín, J.D., Messenger, G., Merino Tomé, O., Suarez-Ruiz, I.,  
756 Razin, P., Grélaud, C., Malaval, M., Joussiaume, R., Hunt, D.W., 2016. Jurassic rifting to post-rift  
757 subsidence analysis in the Central High Atlas and its relation to salt diapirism. Basin Res. 1-27.
- 758 Moragas, M., Vergés, J., Saura, E., Martín-Martín, J.D., Messenger, G., Merino-Tomé, Ó., Suárez-Ruiz, I.,  
759 Razin, P., Grélaud, C., Malaval, M., Joussiaume, R., Hunt, D.W. 2018. Jurassic rifting to post-rift  
760 subsidence analysis in the central High Atlas and its relation to salt diapirism. Basin Research, 30, 336-  
761 362.
- 762 Naji, C., Gharbi, M., Amri, Z., Masrouhi, A., Bellier, O., 2018a. Temporal and spatial changes of the  
763 submarine Cretaceous paleoslope in Northern Tunisia, inferred from slump folds analysis. Proceedings  
764 of the Geologist's Association Volume 129, Issue 1, p. 40-56.
- 765 Naji, C., Masrouhi, A., Amri, Z., Gharbi, M., Bellier, O., 2018b. Cretaceous paleomargin tilted blocks  
766 geometry in northern Tunisia: stratigraphic consideration and fault kinematic analysis. Arabian Journal  
767 of Geosciences, 11, 583.
- 768 Perthuisot, V., Rouvier, H., Smati A., 1998. Style et importance des déformations anté-vraconiennes dans  
769 le Maghreb oriental: exemple du diapir du Jebel Sata. Bulletin de la Société Géologique de France, 8,  
770 389-398.
- 771 Perthuisot, V., Rouvier, H., Smati, A., 1988. Style et importance des déformations anté-vraconiennes  
772 dans le Maghreb oriental: exemple du diapir du Jebel Sata (Tunisie centrale). Bull. Société géologique  
773 France, 4 (8), 391-398.
- 774 Perthuisot., V. 1978. Dynamique et pétrogenèse des extrusions triasiques de Tunisie septentrionale.  
775 Travaux du Laboratoire de Géologie no.12. Presses de l'Ecole Normale Supérieure Paris, 312 p.
- 776 Peybernes, B., Kamoun, F., Durand Delga, M., Thierry, J., Faure, P., Dommergues, J.L., Vila, J.M., Cugny,  
777 P., Ben Youssef, M., 1996. Le Jurassique et le Crétacé basal de la Tunisie nord-occidentale : Essai de  
778 corrélations avec les séries de la dorsale tunisienne et de la « ride » Amar-Djédeida. C. R. Acad. Sci.,  
779 Paris, 323, IIa, 153-162.
- 780 Peybernes, B., Souquet, P., Vila, J.M., Ben Youssef, M., Durand Delga, M., Kamoun, F., Delvolvé, J.J.,  
781 Charrière, A., Ghanmi, M., Zarbout, M., Saadi, J., 1994. Les séries turbiditiques du Tithonien supérieur et  
782 du Crétacé basal (formations Maiana, Hamada et Séroura) de la zone nord-atlasique à « schistosité » (NE  
783 de la Tunisie). C. R. Acad. Sci., Paris, 319, II, 1535-1543.
- 784 Ramos, A., Fernández, O., Muñoz, J.A., Terrinha, P., 2017. Impact of basin structure and evaporite  
785 distribution on salt tectonics in the Algarve Basin, Southwest Iberian margin. Marine and Petroleum  
786 Geology, 88, 961-984.
- 787 Rigo, L., Garde, S., El Euch, H., Bandt, K., Tiffert, J., 1996. Mesozoic fractured reservoirs in a  
788 compressional structural model for north-eastern Tunisia atlasic zone, Entreprise Tunisienne d'Activités  
789 Pétrolières, 10, 233-355.

- 790 Roca, E., Beamud, E., Rubinat, M., Soto, R., Ferrer, O., 2013. Paleomagnetic and inner diapiric structural  
791 constraints on the kinematic evolution of a salt-wall: The Biorb-Quesa and northern Navarrés salt-wall  
792 segments case (Prebetic Zone, SE Iberia). *Journal of Structural Geology*, 52, 80-95.
- 793 Rosenbaum, G., Lister, G. S., Duboz, C., 2002. Relative motions of Africa, Iberia and Europe during Alpine  
794 orogeny. *Tectonophysics*, 359, 117-129.
- 795 Roure, F., Casero, P., Addoum, B., 2012. Alpine inversion of the North African margin and delamination  
796 of its continental lithosphere. *Tectonics*, 31, TC3006.
- 797 Rouvier, H., Henry, B., Le Goff, M., Hatira, N., Laatar, E., Mansouri, A., Perthuisot, V., Smati, A., 1998.  
798 Preuves paléomagnétiques de la non-interstratification des évaporites du Trias dans l'Albien du  
799 Maghreb oriental. *Comptes Rendus de l'Académie des Sciences, Paris* 326 (IIa), 363–368.
- 800 Rowan, M. G., Hearon, T. E., Kernen, R. A., Giles, K. A., Gannaway-Dalton, C. E., Williams, N. J., Fiduk, J. C.,  
801 Lawton, T. F., Hannah, P. T., Fischer, M. P., (2019): A review of allochthonous salt tectonics in the  
802 Flinders and Willouran ranges, South Australia. *Australian Journal of Earth Sciences*, 1–27.
- 803 Rowan, M. G., Lawton, T. F., Giles, K. A., Ratliff, R. A., 2003. Near-salt deformation in La Popa Basin,  
804 Mexico, and the northern Gulf of Mexico: A general model for passive diapirism. *American Association  
805 of Petroleum Geologists Bulletin*, 87, 733-756.
- 806 Rubinat, M., Roca, E., Escalas, M., Queralt, P., Ferrer, O., Ledo, J. J., 2013. The influence of basement  
807 structure on the evolution of the Biorb-Quesa Diapir (eastern Betics, Iberian Peninsula): Contractive  
808 thin-skinned deformation above a pre-existing extensional basement fault. *International Journal of Earth  
809 Sciences*, 102, 1, 25-41.
- 810 Sarsar Naouali, B., Guellala, R., Bey, S., Inoubli, M. H., 2017. Gravity Data Contribution for Petroleum  
811 Exploration Domain: Mateur Case Study (Saliferous Province, Northern Tunisia). *Arabian Journal for  
812 Science and Engineering*, 42, 339–352.
- 813 Saura, E., Ardèvol i Oró, L., Teixell, A., Vergés, J., 2016. Rising and falling diapirs, shifting depocenters,  
814 and flap overturning in the Cretaceous Sopeira and Sant Gervàs subbasins (Ribagorça Basin, southern  
815 Pyrenees), *Tectonics*, 35, 638-662.
- 816 Saura, E., Embry, J. C., Vergés, J., Hunt, D. W., Casciello, E., Homke, S., 2013. Growth fold controls on  
817 carbonate distribution in mixed foreland basins: Insights from the Amiran foreland basin (NW Zagros,  
818 Iran) and stratigraphic numerical modelling, *Basin Res.*, 25, 149-171.
- 819 Saura, E., Garcia-Castellanos, D., Casciello, E., Parravano, V., Urruela, A., Vergés, J., 2015, Modeling the  
820 flexural evolution of the Amiran and Mesopotamian foreland basins of NW Zagros (Iran-Iraq),  
821 *Tectonics*, 34, 377–395.
- 822 Saura, E., Vergés, J., Martín-Martín, J. D., G., M., Moragas, M., Razin, P., Grélaud, C., Jousiaume, R.,  
823 Malaval, M., Homke, S., and Hunt, D., 2014. Syn- to post-rift diapirism and minibasins of the Central High  
824 Atlas (Morocco): the changing face of a mountain belt. *Journal of the Geological Society*, v. 171, no. 1, p.  
825 97-105.
- 826 Schuster, D. C., 1995. Deformation of allochthonous salt and evolution of related salt-structural systems,  
827 eastern Louisiana Gulf Coast, In *Salt tectonics: A global perspective* (eds. Jackson, M. P. A. Roberts, D. G.,  
828 Snelson, S.) pp. 177-198. American Association of Petroleum Geologists Memoir no. 65.
- 829 Slama, M.-M.B., Masrouhi, A., Ghanmi, M., Youssef, M.B., Zargouni, F., 2009. Albian extrusion evidences  
830 of the Triassic salt and clues of the beginning of the Eocene atlastic phase from the example of the

- 831 Chitana-Ed Djebes structure (N.Tunisia): Implication in the North African Tethyan margin recorded events,  
832 comparisons. *Comptes Rendus - Geoscience*, 341, 7, 547-556.
- 833 Soto, J.I., Flinch, J.F., Tari, G., 2017. Permo-Triassic Basins and Tectonics in Europe, North Africa and the  
834 Atlantic Margins: A Synthesis. In *Permo-Triassic Salt Provinces of Europe, North Africa and the Atlantic*  
835 *Margins*, 3-41. Elsevier edition, 2017, 632.
- 836 Soua, M., 2014. Early Carnian anoxic event as recorded in the southern Tethyan margin, Tunisia.  
837 *International Geology Review*, v. 56, no. 15, p. 1884-1905.
- 838 Soumaya, A., Ben Ayed, N., Delvaux, D., Ghanmi, M., 2015. Spatial variation of present-day stress field  
839 and tectonic regime in Tunisia and surroundings from formal inversion of focal mechanisms:  
840 Geodynamic implications for central Mediterranean. *Tectonics*, 34, 6, 1154-1180.
- 841 Souquet, P., Peybernes, B., Saadi, J., Ben Youssef, M., Ghanmi, M., Zarbout, M., Chikhaoui, M., Kamoun,  
842 F., 1997. Séquences et cycles d'ordre 2 en régime extensif et transtensif : exemple du Crétacé inférieur  
843 de l'Atlas tunisien, *Bulletin de la Société Géologique de France*, 168,373-386.
- 844 Soussi, M., Enay, R., Boughdiri, M., Mangold, C., Zaghib-Turki, D., 1999. Ammonitico Rosso (Zaress  
845 Formation) of the Tunisian Dorsale. *Comptes Rendus de l'Academie de Sciences - Serie IIa*: 329(4), 279-  
846 286.
- 847 Soussi, M., Niedźwiedzki, G., Tałanda, M., Drózdź, D., Sulej, T., Boukhalifa, K., Mermer, J., Błazejowski, B.,  
848 2017. Middle Triassic (Anisian-Ladinian) Tejra red beds and Late Triassic (Carnian) carbonate  
849 sedimentary records of southern Tunisia, Saharan Platform: Biostratigraphy, sedimentology and  
850 implication on regional stratigraphic correlations. *Marine and Petroleum Geology*, 79, 222-256.
- 851 Talbot, C.J., 1993. Spreading of salt structures in the Gulf of Mexico: *Tectonophysics*, 228, 151-166.
- 852 Talbot, C.J., 1998. Extrusions of Hormuz salt in Iran, In *the Past is the Key to the Present: (Eds Blundell,*  
853 *DJ., Scott, AC.)* pp. 315-334. Geological Society of London, Special Publications no 143.
- 854 Talbot, C.J., Rönnlund, P., Schmeling, H., Koyi, H., Jackson, M.P.A., 1991. Diapiric spoke patterns.  
855 *Tectonophysics*, 188, 187-201.
- 856 Truillet, R., Delteil, J., 1982. Allochtonie alpine de la « zone des diapirs » de Tunisie septentrionale et du  
857 Nord-Est algerien, *C. R. Acad. Sci., Ser. II* 294, 1143–1146.
- 858 Van Hinsbergen, D., Vissers, R., Spakman, W., 2014. Origin and consequences of western Mediterranean  
859 subduction, rollback, and slab segmentation. *Tectonics*, 33, 4, 393-419.
- 860 Vendeville, B.C., Jackson, M.P.A., 1992b. The fall of diapirs during thin-skinned extension. *Marine and*  
861 *Petroleum Geology*, 9, 354-371.
- 862 Vergés, J., Sàbat, F., 1999. Constraints on the Neogene Mediterranean kinematic evolution along a 1000  
863 km transect from Iberia to Africa. Geological Society, London, Special Publications, 156, 63-80.
- 864 Vila, J. M., 1995. Première étude de surface d'un grand 'glacier de sel' sous-marin: l'est de la structure  
865 Ouenza-Ladibel-Meridef (confins algéro-tunisiens). Proposition d'un scénario de mise en place et  
866 comparaisons. *Bulletin de la Société Géologique de France*, 166, 149-167.
- 867 Vila, J. M., Sigal, J., Coiffait, P. E., Lahondère, J. C., Quinif, Y., 1975. Sur l'allochtonie du Tell sétifien: La  
868 fenêtre de la Koudiat Touachra et la nappe de Djemila, *Bull. Soc. Geol. France*, 17, 1173-1175.
- 869 Vila, J.M., Ben Youssef, M., Charrière, A., Chikhaoui, M., Ghanmi, M., Kamoun, F., Peybernes, B., Saadi, J.,  
870 Souquet, P., Zarbout, M., 1994. Découverte en Tunisie, au SW du Kef, de matériel triasique interstratifié

- 871 dans l'Albien : extension du domaine à « glaciers de sel » sous-marins des confins algéro-tunisiens.  
872 Comptes Rendus à l'Académie des Sci. Paris 318 (II), 1661-1667.
- 873 Vila, J.M., Ben Youssef, M., Chikhaoui, M., Ghanmi, M., 1996. Un grand 'glacier de sel' sous-marin albien  
874 du Nord-Ouest tunisien (250 km<sup>2</sup>): le matériel salifère triasique du « diapir » de Ben Gasseur et de  
875 l'anticlinal d'El Kef. Comptes Rendus de l'Académie des Sciences Paris, 322, 221-227.
- 876 Vila, J.M., Ghanmi, M., Ben Youssef, M., Jouirou, M., 2002. Les 'glaciers de sel' sous-marins des marges  
877 continentales passives du nord-est du Maghreb (Algérie-Tunisie) et de la Gulf Coast (USA):  
878 comparaisons, nouveau regard sur les 'glaciers de sel' composites, illustre par celui de Fedj el Adoum  
879 (Nord-Ouest tunisien) et revue globale. *Eclogae Geologicae Helveticae*, 95, 347-380.
- 880 Warsitzka, M., Jähne-Klingberg, F., Kley, J., Kukowski, N., 2019. The timing of salt structure growth in the  
881 Southern Permian Basin (Central Europe) and implications for basin dynamics. *Basin Research*, *Basin*  
882 *Res.*, 31, 337-360.
- 883 Weijermars, R., Jackson, M.P.A., Vendeville, B., 1993. Rheological and tectonic modeling of salt  
884 provinces. *Tectonophysics*, 217, 143-174.
- 885 Wu, S., Bally, A.W., Cramez, C., 1990. Allochthonous salt, structure and stratigraphy of the north-eastern  
886 Gulf of Mexico: Part II. Structure: *Marine and Petroleum Geology*, 7, 334-370.
- 887 Yin, H., Zhang, J., Meng, L., Liu, Y., Xu, S., 2009. Discrete element modeling of the faulting in the  
888 sedimentary cover above an active salt diapir. *Journal of Structural Geology*, 31, 989-995.
- 889 Zargouni, F., 1975. Etude géologique de la chaîne de Lansarine (région de Tébourba, Atlas tunisien). PhD  
890 thesis (Thèse 3ème cycle), Pierre-et-Marie-Curie University (Paris VI), 86 p. Published thesis.
- 891 Zouaghi, T., Bédir, M., Ayed-Khaled, A., Lazzez, M., Soua, M., Amri, A., Inoubli, M.H., 2013.  
892 Autochthonous versus allochthonous upper triassic evaporites in the sbiba graben, central Tunisia.  
893 *Journal of Structural Geology*, 52, 1, 163-182.
- 894 Zucker, E., Frumkin, A., Agnon, A., Weinberger, R., 2019. Internal deformation and uplift-rate of salt  
895 walls detected by a displaced dissolution surface, Dead Sea basin. *Journal of Structural Geology*,  
896 127,103870.
- 897
- 898

899 **Figure captions**

900 Figure 1: (a) Geodynamic setting of the Maghreb fold-thrust-belt and location of north Tunisian domain.  
901 (b) Simplified sketch of the Tunisian Atlas showing the major tectonic units, major thrust systems, main  
902 outcropping Triassic salt and the location of the LBSS.

903 Figure 2: Stratigraphy of the north Tunisian domain with indication of average thickness variation,  
904 lithostratigraphic short description, the average density of main units and the regional tectonic regime.

905 Figure 3: Detailed geological map of the LBSS and its surrounding areas showing the main units, their  
906 relationships, the Triassic salt shape, the location of the detailed maps of figs 4 and 5 and the location of  
907 seismic profiles of figs 8-10.

908 Figure 4: Detailed geological map of the northern part of the LBSS showing the salt contact, the main  
909 outcrops of Cretaceous that constitutes the bedrock of the large salt canopy, and fault kinematics  
910 analysis of few fault sites highlighting a major NW-SE Cenozoic compression.

911 Figure 5: Detailed geological map of the central part of the LBSS showing the salt contact, the main  
912 outcrops of Cretaceous that constitutes the bedrock of the large salt canopy (Ain el Karma) and the  
913 cover of the Triassic salt (Jebel Djedaria), under the thrust systems of the Lansarine structure.

914 Figure 6: Panoramic view looking northeastward of the Jebel Djedaria structure shows the configuration  
915 and reproduces the geological history of this region with (a) uninterpreted and (b) interpreted section.  
916 In the south, the Triassic is covered by normal polarity Cretaceous sequences, themselves  
917 unconformably covered by Oligocene–Lower Miocene (15-20° angular Atlassic unconformity). The  
918 Oligocene–Lower Miocene sequences are overthrust by southeast-verging the Lansarine nappe  
919 formed by Paleocene shale and Eocene limestone.

920 Figure 7: fault kinematics analysis of abundant meso-scale synsedimentary faults within the Cretaceous  
921 sequences. The Stereonets are back-tilted faults that indicate a NE-SW Aptian–Albian tectonic extension;  
922 E-W to NE-SW late Cretaceous tectonic extension; and Santonian NW-SE to N-S tectonic extension.

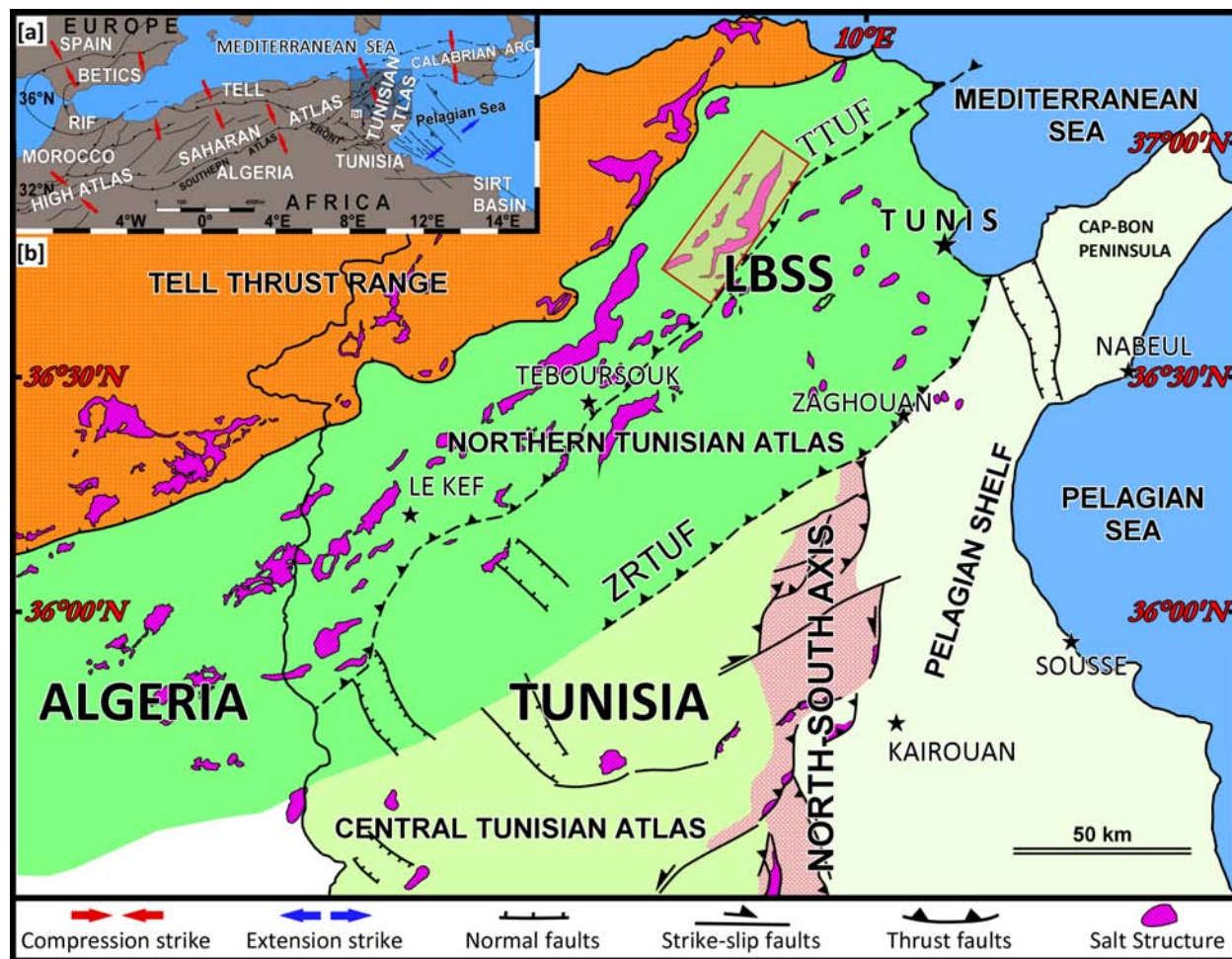
923 Figure 8: (a) Uninterpreted, migrated, depth-converted seismic reflection data from the LBSS area. (b)  
924 Interpreted seismic line of L18A and L18B showing the preserved extensional Chouigui mini-basin to the  
925 south associated with the major Teboursouk thrust fault. Note that the thrust fault systems are  
926 connected to intra-basement detachment normal fault. The salt sheet covers a Cretaceous sequences at

927 depth. Under Lansarine structure the velocity and the shape of reflectors seem to highlight a salt body  
928 (Lansarine diapir). The thrust fault is connected at depth to rollover anticline limited by the listric normal  
929 fault connected to the intra-basement detachment all of them are inverted structures.

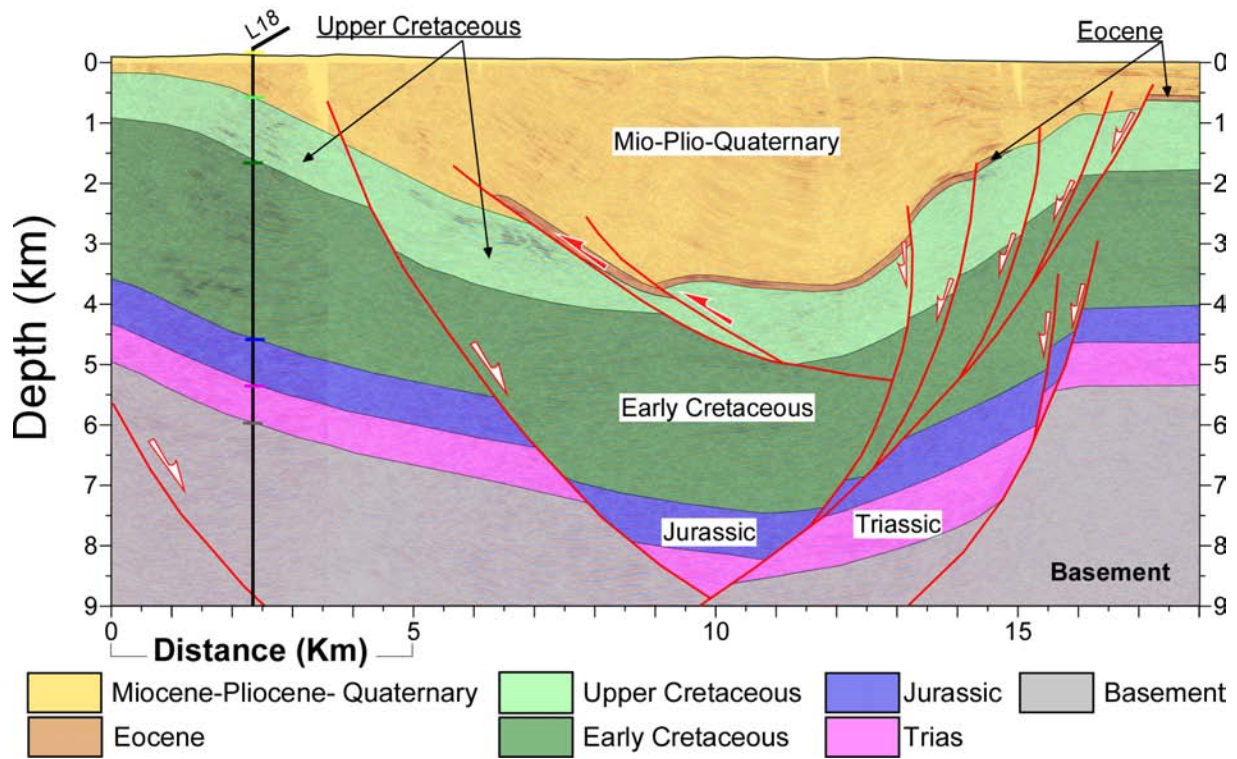
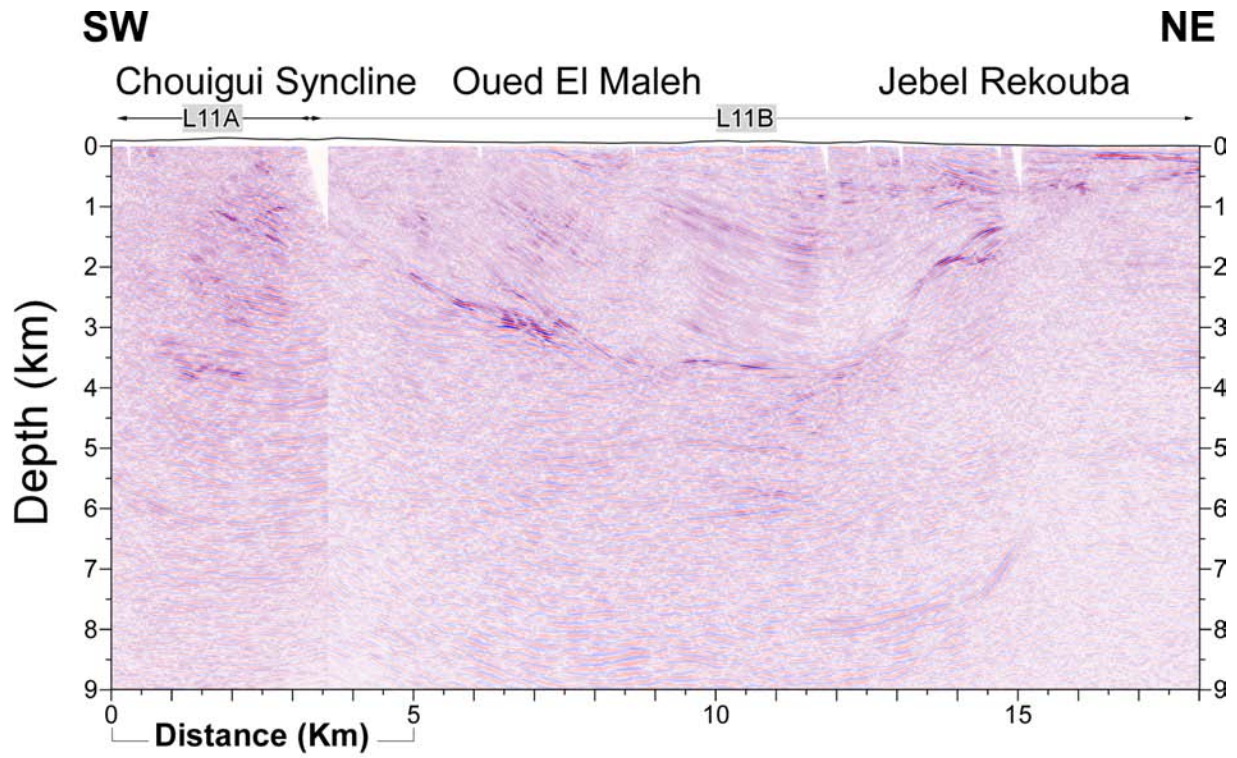
930 Figure 9: seismic section L05 crosses the northern domain. It mainly shows an extensional geologic  
931 setting in this area with the low angle fault systems characterizing the extensional late Miocene collapse  
932 associated to high-angle faults producing a geometry characterized by half-graben and hanging-wall  
933 syncline basins

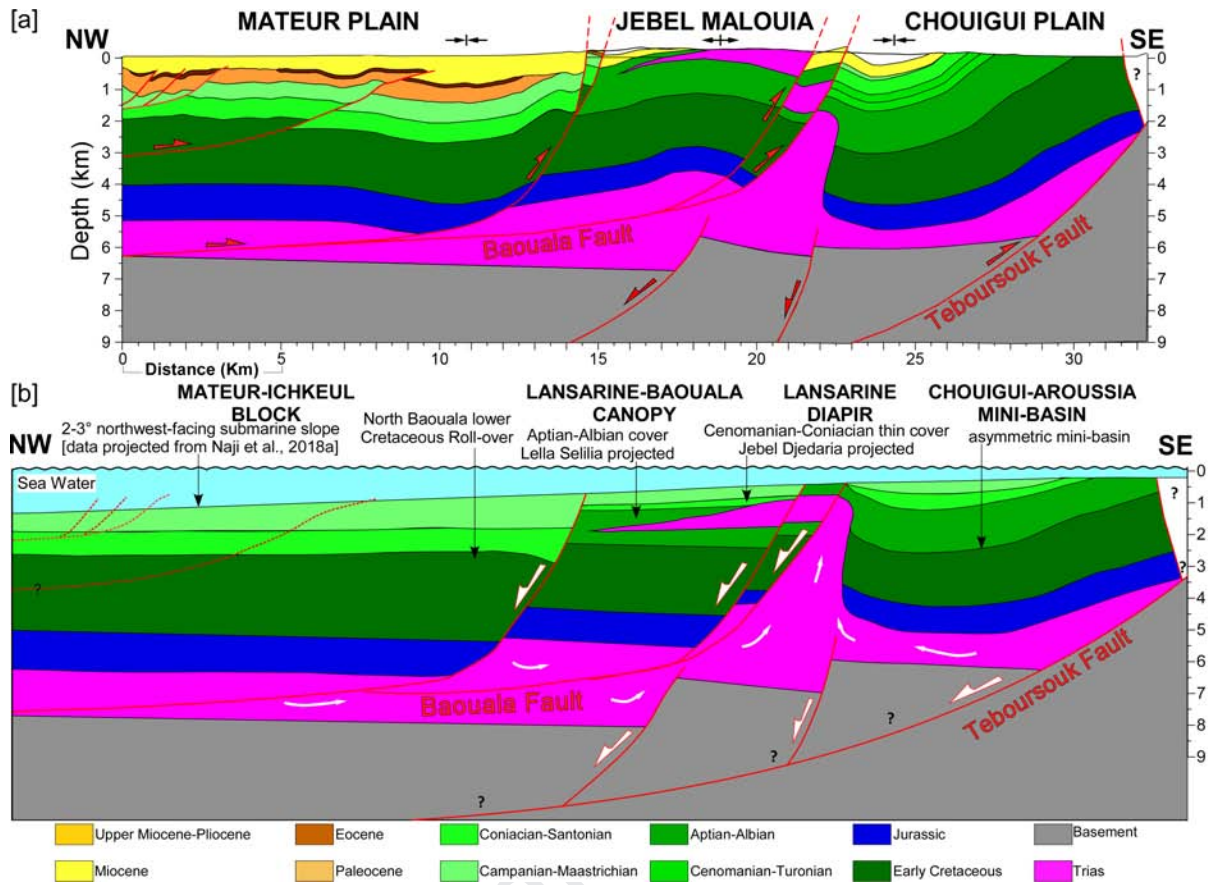
934 Figure 10: NE-SW seismic line L11 located in the front of the thrust systems of LBSS showing a narrow  
935 basin filled by Mio-Plio-Quaternary sediments reached a 3 km and mainly recorded by Miocene  
936 syntectonic strata. The high angle connected normal faults and the sequences in this narrow basin are  
937 interpreted as an orthogonal extension in which the thrust strongly influences the development of  
938 normal faults.

939 Figure 11: simplified Palinspastic stages reconstruction cross-section. (a) Present-day. (b) Late  
940 cretaceous state. Shortening amount is hypothesized to be  $\pm 6.5$  km ( $\sim 17-18\%$ ). See text for detail on  
941 halotectonics stages and styles.



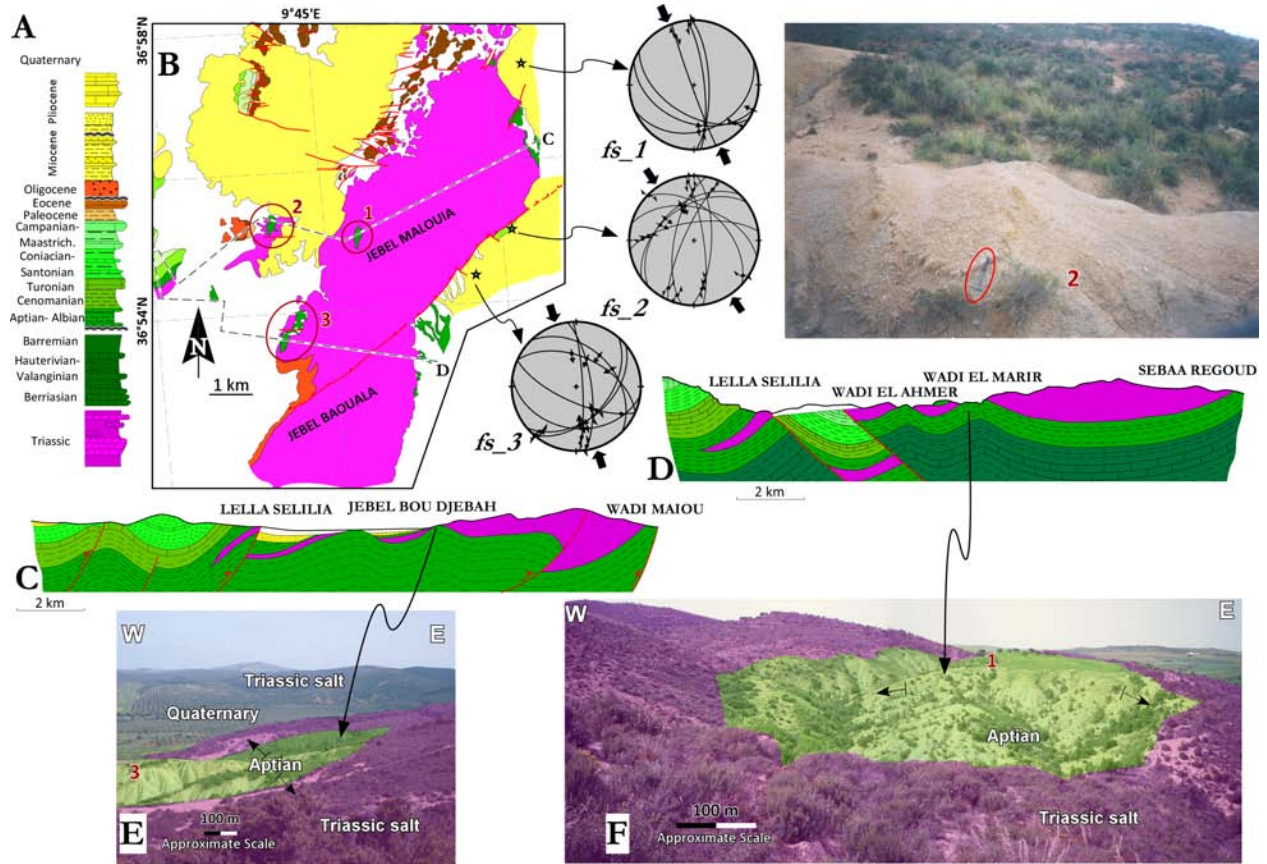


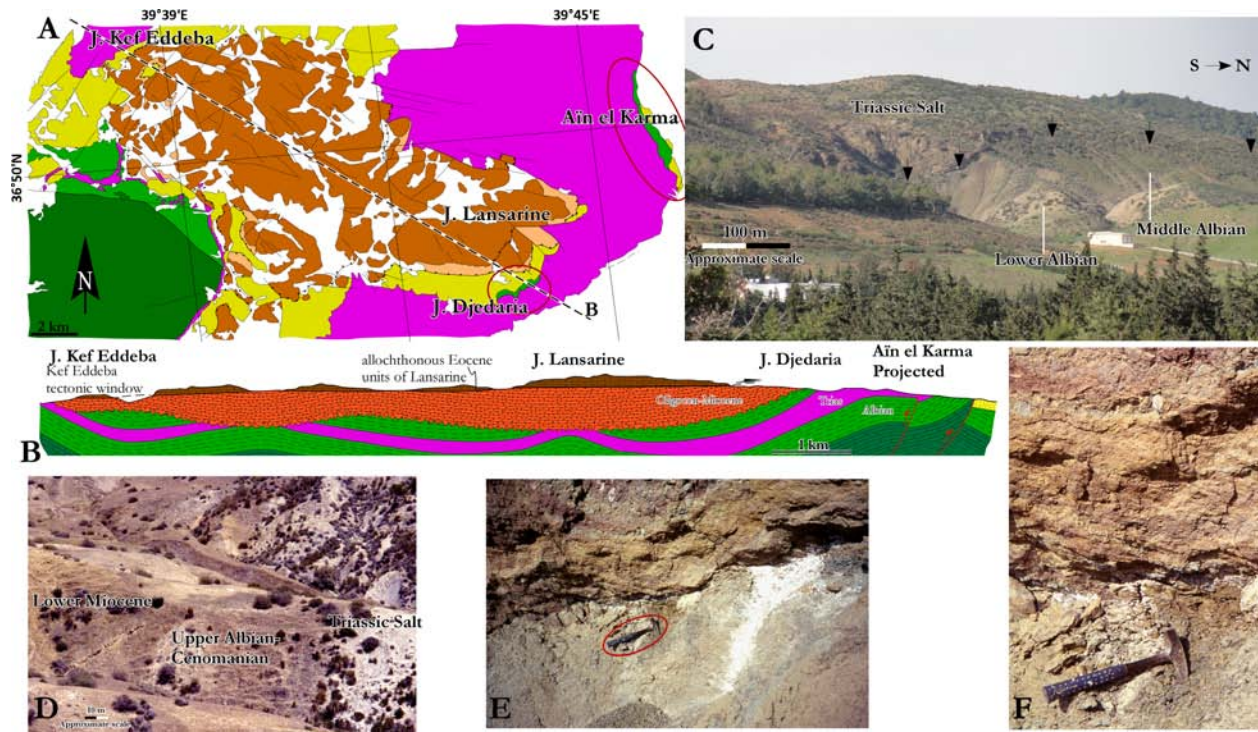


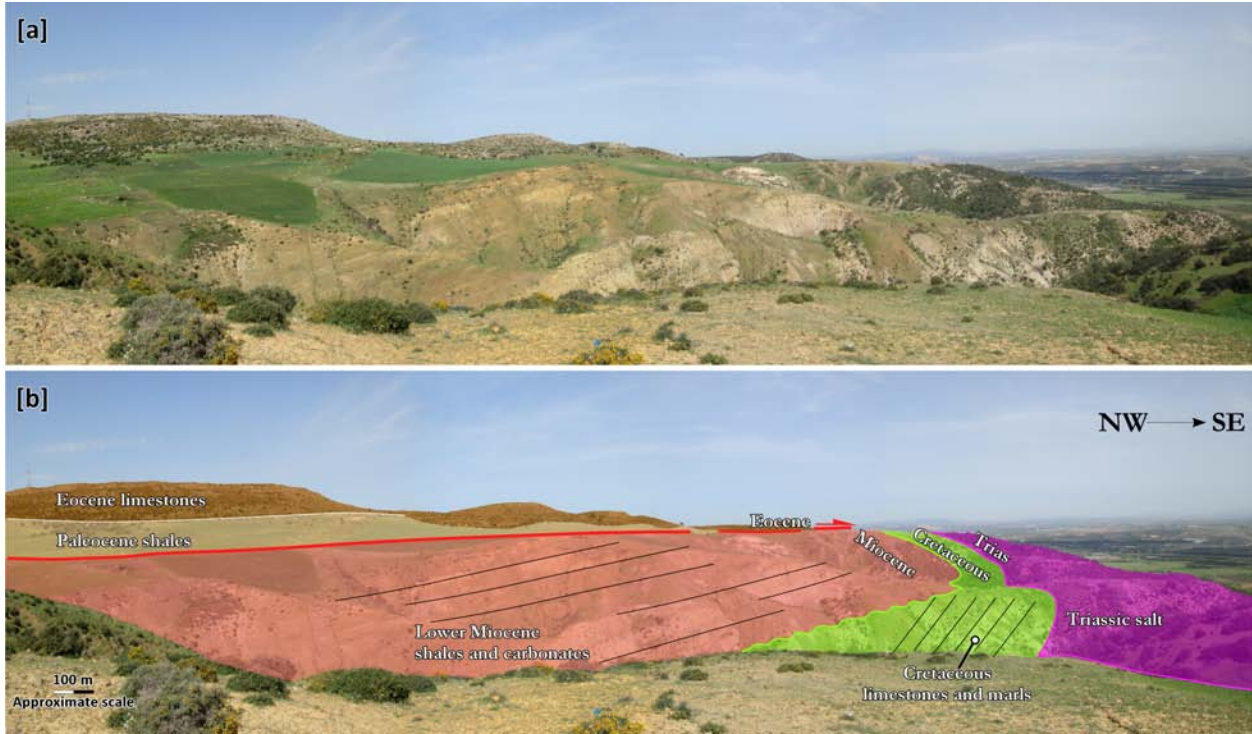


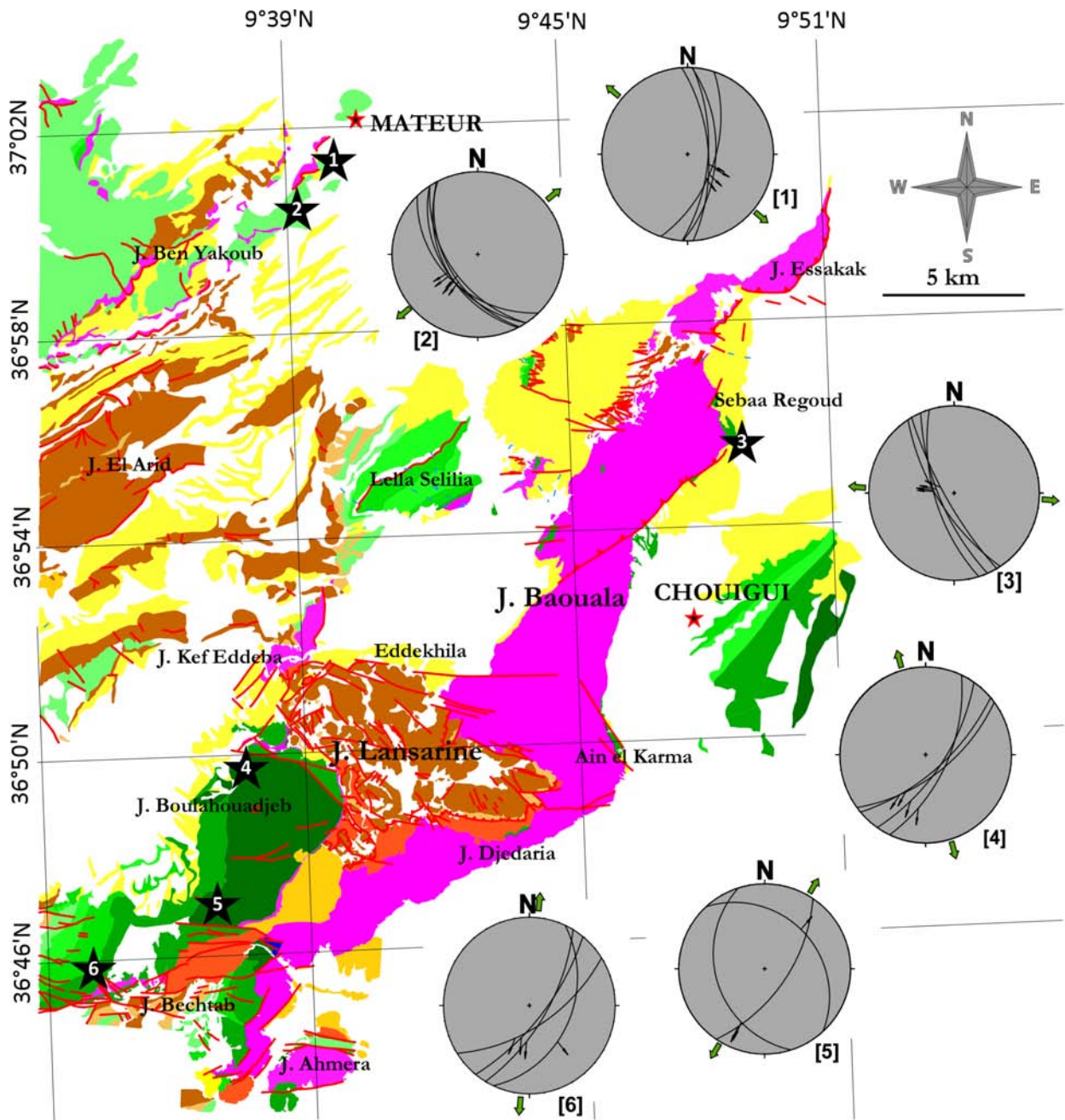
Age	Lithology and Density g/cm <sup>3</sup>	Thickness variation	Lithostratigraphical description	Regional Tectonic	
Quaternary		2.05	0–100 m	Soil	
Pliocene		2.60	250–370 m	Sands and sandstones with rare clays intercalations	
Miocene	Messinian		150–300 m	Black clays with lacustrine marls and gypsum	
	Serrevalian-Tortonian	2.60	500–2700 m	Gray clays and marls with rare sandy intercalation Sandstones and sandy marls with evaporitic intercalation and gypsum sequences	
Paleogene	Oligocene	2.58	0–50 m	Siliceous grainstone	
	Upper Eocene	2.62	50–100 m	Siliceous yellowish limestones	
	Paleocene	2.62	800–1000 m	Dark marls	
Cretaceous	Campanian-Maastrichtian	2.53	60–160 m	Marine limestones and claystones presented by two carbonate members	
	Coniacian-Santonian	2.52	350–900 m	Thick sequences of marls-limestone with marls dominance	
	Turonian	2.54	60–200 m	Marls and limestones alternation	
	Aptian-Albian	2.63	100–1000 m	Black limestones and green black marls Black to green marls with calcareous layers	
	Barremian	2.63	450–700 m	Marls and dark nodular limestones alternations	
	Hauterivian-Valanginian	2.62	130–800 m	Marls with limestones and frequents sandstones alternations	
	Berriasian		60 m	Greenish muds and thin bedded sandstones and siltstones	
	Jurassic		2.58	40–440 m	Carbonates composed of calcites and dolomites Dark carbonates with marble aspect and red to dark brown pelites with siliceous limestones beds
Triassic		2.17	150–1000 m	Thick continental evaporitic salt (halite-gypsum), clays and dolomites	



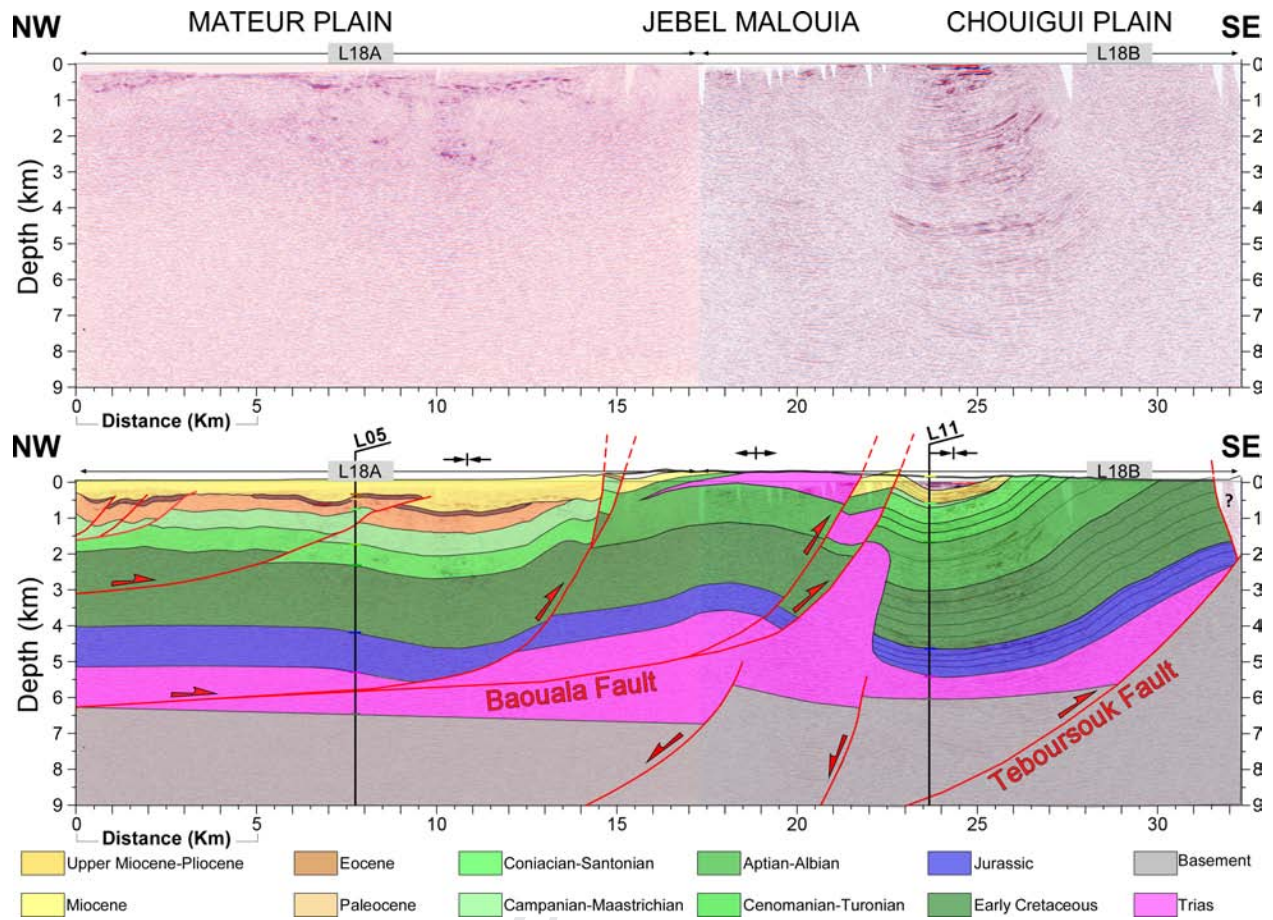


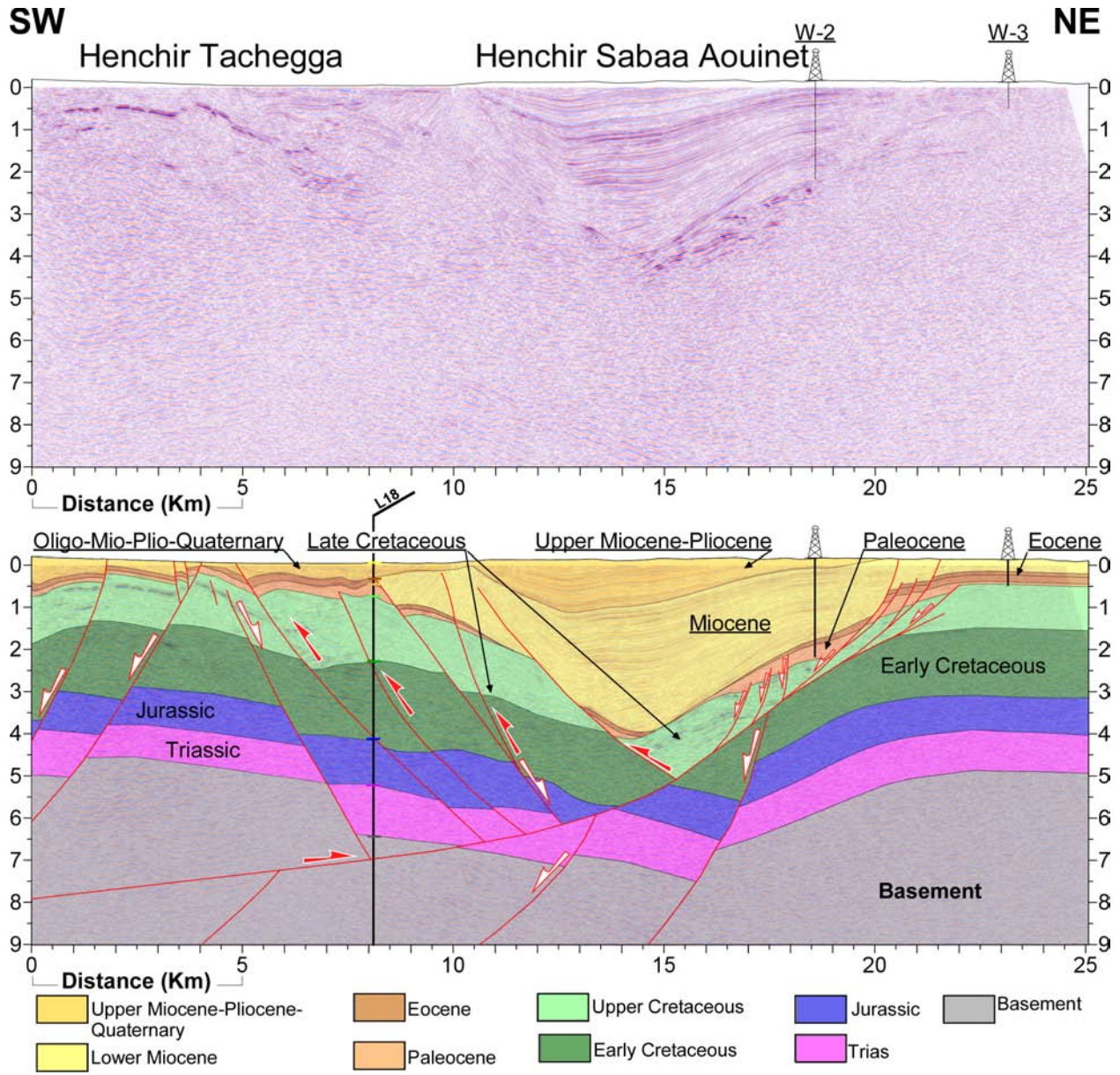












### **Highlights**

Active Salt diapir developed during Tethyan Mesozoic extension in Northern Tunisia

Significance of allochthonous salt sheets spreading laterally from the diapir stem

During subsequent compressional stage diapir is squeezed and passively transported above major thrust

Journal Pre-proof